Composite Recycling with Biocatalytic Thermoset Reforming

Clarissa Olivar,[‡] Zehan Yu,[#] Ben Miller,[‡,v] Maria Tangalos,[‡,v] Cory B. Jenkinson,[||] Steven R. Nutt,[#] Berl R. Oakley,[||] Clay C. C. Wang,[‡,v,*] Travis J. Williams[‡,*]

[‡]Department of Chemistry, Donald P. and Katherine B. Loker Hydrocarbon Institute, and Wrigley Institute for Environment and Sustainability, University of Southern California, Los Angeles, California 90089, United States

[#]Department of Chemical Engineering & Materials Science and M.C. Gill Composites Center, University of Southern California, Los Angeles, California 90089, United States

[v]Department of Pharmacology & Pharmaceutical Sciences, University of Southern California, Los Angeles, California 90089, United States

[||]Department of Molecular Biosciences, University of Kansas, Lawrence, Kansas 66045, United States

ABSTRACT: Carbon fiber reinforced polymers (CFRPs, or composites) are increasingly replacing traditional manufacturing materials used in the automobile, aerospace, and energy sectors. With this shift, it is vital to develop end-of-life processes for CFRPs that retain the value of both the carbon fibers and the polymer matrix. Here we demonstrate a strategy to upcycle pre- and post-consumer polystyrene-containing CFRPs, crosslinked with unsaturated polyesters or vinyl esters, to benzoic acid. The thermoset matrix is upgraded via biocatalysis utilizing an engineered strain of the filamentous fungus *Aspergillus nidulans*, which gives access to valuable secondary metabolites in high yields, exemplified here by (2Z,4Z,6E)-octa-2,4,6-trienoic acid. Reactions are engineered to preserve the carbon fibers, with much of their sizing, so that the isolated carbon fiber plies are manufactured into new composite coupons that exhibit mechanical properties comparable to virgin manufacturing substrates. In sum, this represents the first system to reclaim high value from both the fiber fabric and polymer matrix of a CFRP.

Carbon fiber reinforced polymers (CFRPs) are composite materials comprising carbon fibers embedded in a polymer matrix, commonly a thermosetting polymer such as an epoxy,[1–3] unsaturated polyester,[4,5] or vinyl ester[6] system crosslinked with vinyl monomers, the latter acting as a reactive diluent, processing aid, and catalyst.[7,8] CFRPs are attractive manufacturing materials in the energy, aerospace, and automotive sectors[1–3,9] because of their high strength- and stiffness-to-weight ratios and resistance to corrosion, moisture, and chemical pollutants.[10] CFRPs are generally landfilled at end-of-life because the strong three-dimensional crosslinking network of the polymer matrix makes recycling difficult and repairs impractical.[1–3,9] By 2030, 6,000-8,000 CFRP commercial aircraft will reach their end of service,[11] and by 2050, the retirement of wind turbines will have generated 483,000 tons of CFRP waste, while the demand for carbon fibers and CFRPs is projected to reach 190 kilotons.[10,11] It is therefore imperative to establish viable recycling methods for these composites.

Current options for CFRP recycling include mechanical, thermal, and chemical processes.[1] Mechanical recycling involves shredding CFRPs into smaller pieces, destroying the value in the continuous fiber. Thermal recycling involves energy-intensive pyrolysis (≥ 450 ºC) in which the polymer matrix is discarded as valueless oils and gases, and the high temperatures degrade the mechanical properties of the fibers. Emerging chemical recycling methods, mainly comprising solvolysis of epoxy systems, are attractive when effective chemistries can be found, as some harvest the matrix as valuable chemicals while recovering fibers and retaining the fabrics' architecture and its mechanical properties.[1,12] Here, we show an upcycling chemistry new to the composite space in which tandem chemical and biocatalysis are used respectively to cleave and upgrade a polyolefin-containing composite matrix to high-value products, the first approach to use a waste composite matrix as a manufacturing substrate for fine chemicals.

We exhibit our method on polyester and vinyl ester thermosets. These materials feature durability, low cost, effective fiber-matrix adhesion, and negligible composite shrinkage.[10] Such materials are commonly crosslinked by vinyl monomer polymerization; our case features styrene, as it is both economical and has attractive properties, such as a low molecular weight, high reactivity, and easy processing.[8] Polystyrene (PS)-containing composites are not limited to CFRPs;[13] there is an increasing effort to incorporate post-consumer PS, other organics,[14,15] and natural fibers into composites.[16,17]

Partenheimer established conditions for homogeneous liquid phase aerobic oxidation of polystyrene to benzoic acid utilizing a system comprising acetic acid and metal/bromide catalysts in high yields (≤ 88%).[18] Oxidative methods utilizing

acetic acid and hydrogen peroxide enabled the recovery of both the carbon fibers and resin system

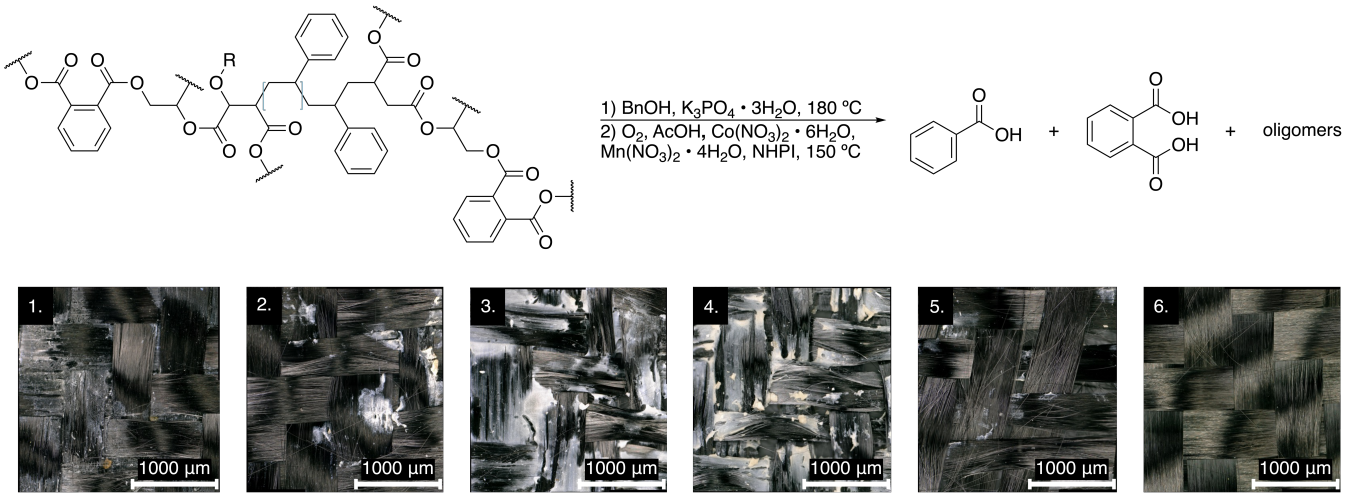

Figure 1. Top: proposed reaction for CFRP digestion. Bottom: resulting carbon fibers from the digestion of pre-consumer CFRPs. Reaction conditions were optimized to obtain clean carbon fiber plies that retained their plain weave pattern and are summarized in Table S4

via formation of peracetic acid in situ as demonstrated by Varughese,[19] while recovery of value from both the fiber and matrix utilizing transition metal catalysts in post-consumer composites was demonstrated by Skrydstrup.[20] Beckham illustrated a tandem biocatalytic method to convert polymer waste into small molecules via bacterial metabolism.[21] Taking inspiration from this work, our composite matrix cleavage proceeds in two steps: (1) presoaking the composite in benzyl alcohol and tripotassium phosphate trihydrate and (2) digestion with manganese(II) and cobalt(II) nitrate salts. We first used CFRP panels featuring a FiberGlast Part #77 polyester molding resin. To measure the composition of both the materials, the matrix was first digested with sulfuric acid and hydrogen peroxide at 100 °C, separating the polymer matrix from the fibers. This provides an accurate quantification of fiber versus polymer content (Tables S1-S3).

In the first step, composite panels (50.8 x 38.1 mm) are incubated in benzyl alcohol and $K_3PO_4 \bullet 3H_2O$ for 24 hours at 180 °C. This appears to swell the composite and enables more facile intercalation of the reagents of the subsequent step. While we used a similar approach with neutral benzyl alcohol when cleaving epoxy composites by catalytic oxidation,[2,12] here we add a base to cleave the polyester crosslinks. The swelling and disconnection are visible, as the pretreatment causes matrix cracking near the surface, yielding a white crystalline substance on the surface of the carbon fiber plies. Infrared spectra of the crystalline material and clear-yellow benzyl alcohol solution resulting from the pretreatment reveal that only the resulting solid contains esters (Figure S13).

Initial attempts at oxidative matrix cleavage (vide infra) without pretreatment involving smaller panels (25.4 mm x 25.4 mm) and a catalyst loading of 4-7 wt% (relative to the composite) for metal catalysts and NHPI yield clean carbon fibers; however, with larger composites suitable for remanufacture, only partial digestion of the matrix is achieved (Table S4, entry 1), thus justifying the added step.

The solvolysis product, pretreated polymer still affixed to the fibers, is further processed with conditions we introduced for converting PS to benzoic acid.[22] We adapt these conditions to yield clean carbon fiber plies that retain their plain weave pattern, which are visually observed and easily imaged via light microscopy (Figure 1). Optimization of reaction conditions are summarized in Table S4. Notably, $K_3PO_4 \bullet 3H_2O$ is required for complete digestion, an observation evident when comparing entries 2 and 6 in Table S4. Increasing the reaction time and amount of acetic acid in the reaction mixture leads to more complete digestion with lower catalyst loading. However, this formulation can leave residual polymer matrix on the fibers (Table S4, entry 5). Characterization via ^{1}H NMR reveals that all entries in Table S4 produce benzoic acid, phthalic acid, and oligomers of different chain lengths (Figures S15-S22).

The reaction conditions in Table S4, entry 6 yield a clean fiber fabric and are used to isolate benzoic acid for fungal upgrading. Using these conditions, benzoic acid is isolated in yields of 93-102% relative to the polystyrene content in the composite. Although most of the benzoic acid yield is attributed to polystyrene conversion, some of the yield can be credited to the conversion of residual benzyl alcohol[23] remaining in the composite after pretreatment, even with thorough washing with acetone. Similar reaction conditions are applied to post-consumer CFRPs (50.8 x 38.1 mm) consisting of polystyrene crosslinked with vinyl esters and chopped, unaligned carbon fibers. This results in a yield of 16-25% for benzoic acid. The complete isolated and recovered composition for pre- and post-consumer composites is summarized in Table S5.

Prior to upgrading, the crude oxidation product is purified via a series of filtrations, extractions, and crystallizations to remove the oligomers and phthalic acid as although phthalic acid does not inhibit growth, it cannot be metabolized by the fungi.[22] Although the final purification step of recrystallizing benzoic acid removes most of the remaining oligomers in the

sample, a yellow impurity co-crystallizes

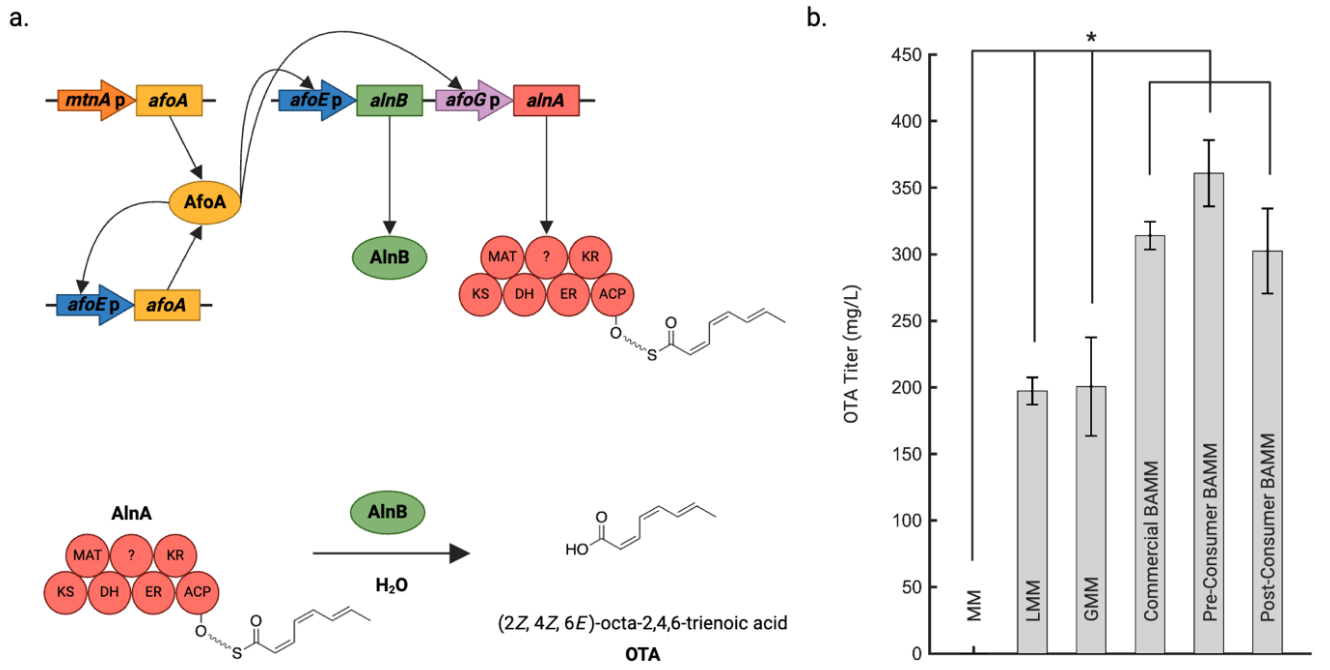

Figure 2. (a) Schematic of the genetic design of LO11055 and biosynthesis of OTA. The promoter of AN11489, which we identify as a metallothionein gene and hereby designate *mtnA*, was inserted to constitutively express AN1029 (*afoA*), whose gene product, AfoA, is a strong transcription factor. AN11191 (*alnA*) and AN11199 (*alnB*) produce AlnA and AlnB, the two proteins responsible for OTA synthesis, were placed under the control of the AN1036 promoter [*afoG*(p)] and the AN1034 promoter [*afoE*(p)], respectively. AfoA binds to these promoters to drive transcription of *alnA* and *alnB*. Additionally, a copy of *afoA* under control of *afoE*(p) was inserted, creating positive feedback. (b) Comparative OTA production by medium type where MM: minimal medium, LMM: lactose minimal medium, GMM: glucose minimal medium, BAMM: benzoic acid minimal medium. Commercial BAMM was created using commercially sourced benzoic acid, whereas Pre-Consumer and Post-Consumer BAMM were created using benzoic acid derived from pre-consumer and post-consumer composite materials. OTA titers were quantified using HPLC-DAD. Bars represent means and error bars represent standard deviations. *p<0.05.

with the product and is detected by elemental analysis (Table S6). The impurity does not inhibit fungal upgrading.

We previously upgraded PS-derived benzoic acid to secondary metabolites via the model fungal organism *Aspergillus nidulans*,[22] wherein polymer digest was the sole carbon source. This, in conjunction with its diverse secondary metabolite profile, makes *A. nidulans* the ideal candidate for the biochemical upcycling of CFRP-derived benzoic acid into a valuable fungal metabolite. Here, we upgrade the composite matrix to (2Z,4Z,6E)-octa-2,4,6-trienoic acid, OTA. OTA is an intermediate in the biosynthetic pathway for (+)-asperlin, a molecule with antitumor, antibiotic, and anti-inflammatory properties.[24,25] OTA is of particular interest because its conjugated backbone readily lends itself as a potential feedstock compound with synthetic chemistry applications,[26] such as ketonization, Kolbe coupling, and olefin coupling. Thus, we demonstrate here the formation of a versatile platform chemical from a waste stream of industrial scale.

In *A. nidulans*, the production of OTA requires the expression of two genes, *alnA* (AN11191 using the FungiDB.org gene designation), which is a polyketide synthase (PKS) and *alnB* (AN11199) that is thought to be required for the release of OTA from the PKS. We previously developed an OTA-producing strain, LO4912, by replacing the native promoters of *alnA* and *alnB* with a regulatable *alcA* promoter.[25] To achieve higher yields and eliminate the need for induction, we engineered a strain with a strong constitutive promoter system that employs a positive feedback loop, after our recent success with a similar system in the production of the fungal secondary metabolite asperbenzaldehyde.[22] In the resultant strain, LO11055, the feedback loop promotes the expression of *alnA* and *alnB*, which drives OTA biosynthesis (Figure 2a).

Thus, we use LO11055 for the biosynthetic conversion of CFRP-derived benzoic acid into OTA. In a representative experiment, LO11055 is inoculated into liquid minimal media (MM) containing 10 g/L of glucose (GMM), 15 g/L of lactose (LMM), or 10 g/L of benzoic acid obtained commercially, isolated from

a pre-consumer composite source or isolated from a post-consumer composite source. A minimal medium without a carbon source is used as a negative control. We find that LO11055 successfully utilizes benzoic acid from all three sources to grow and produce OTA. The OTA yield is determined via HPLC-DAD with statistical significance quantified by the unpaired t-test (Figure 2b). Notably, three benzoic acid sources (commercial, FiberGlast Part #77-derived, and post-consumer-derived) yield OTA at statistically significant higher yields than either GMM or LMM. This was surprising given that LMM and GMM, in particular, are excellent carbon sources that support rapid growth. Benzoate utilization in *A. nidulans* has been studied extensively, however,[27,28] and the results may give clues as to why benzoic acid is converted more efficiently into OTA than glucose or lactose. Benzoate is converted by benzoate *para*-hydroxylase into *para*-hydroxybenzoate, which is, in turn, converted to protocatechuic acid.[27–29] Protocatechuic acid is converted to 3-oxyadipate which feeds into the TCA/glyoxylate cycle. Oxaloacetate from the TCA cycle is converted by AcuF to phosphoenylpyruvate which is converted to pyruvate which is converted to acetyl-CoA. Acetyl-CoA is converted to malonyl-CoA by acetyl-CoA carboxylase. Acetyl-CoA and malonyl-CoA are the building blocks of polyketides, and the structure of OTA indicates that it is synthesized from four malonyl-CoA molecules. We speculate, therefore, that the greater yields of OTA on benzoic acid than glucose or lactose are due to benzoic acid being converted to malonyl-CoA by a mechanism that bypasses the longer glycolytic pathway that converts carbohydrates such as lactose or glucose into pyruvate. All carbon-source containing conditions also outperform previously reported bacterial-biosynthesized OTA yields by 172-185%.[26] The elevated yields of OTA associated with composite-derived benzoic acid as the sole carbon source are promising results that hold up the stepwise chemical/biocatalytic approach as a new and productive paradigm to upcycling composite polymers not yet touched by modern methods for epoxy recovery.

Many reports of composite recycling schemes recover fibers, but few show their utility as manufacturing substrates. We imaged our recovered carbon fibers, rCF, via scanning electron microscopy (Figures S3-S7) after cleaning them following the procedure described in the supplemental information. These rCFs appear clean and free of surface damage. X-ray photoelectron spectroscopy (XPS) reports the change in the surface chemistry of the fibers after recycling (Figures S8-S10 and Table S7). XPS data shows that sizing functionalities, such as hydroxyl and carboxyl groups, diminish but do not disappear during recycling. We restore diminished sizing by employing a nitric acid treatment, as shown in Figure S10.

Single-fiber tensile strengths of virgin and recovered CFs were measured and summarized in Figure S11 and Tables S8-S10. We find that rCFs retained > 97% of the tensile strength and > 99% of the modulus of virgin fibers. Cleaned but not resized rCFs are readily remanufactured into a second-generation composite with aerospace-grade resin films, cured through a vacuum bag only (VBO, non-autoclave) process. Cross sections of the second-generation composite were polished and examined by light microscopy (Figure S12). The second-generation composite is well consolidated, demonstrating the viability of upcycling intact carbon fiber fabrics under the proposed conditions.

The production of both OTA and a second-generation composite coupon from the same starting CFRP sample illustrates the first case of remanufacturing both the CFRP polymer matrix and reinforcing fibers, the latter without disruption of alignment or pattern. While minimal disruption of sizing is observed by XPS, the fabric is remanufactured directly or readily resized with nitric acid. Thus, we provide the first method that fully recovers value from both fiber and matrix components of pre- and post-consumer polystyrene containing CFRPs. The procedure is not only rapid, occurring within one week, but also results in high yields of OTA, 172-185% more than previous reports utilizing bacteria instead of fungi. Recovered carbon fibers are readily used to produce a second-generation composite with negligible loss of material properties and minimal, reversible changes to the fibers' surface chemistry.

ASSOCIATED CONTENT

Supporting Information

The Supporting Information is available free of charge on the ACS Publications website.

Procedures for optimization of reaction conditions, compound and recovered fiber purification, media recipes and fungal metabolism, *Aspergillus nidulans* strain engineering, NMR spectra and chemical shift data, IR spectra, UV-vis spectrum, XPS spectra, SEM images. (PDF)

AUTHOR INFORMATION

Corresponding Authors

Clay C. C. Wang – Department of Pharmacology & Pharmaceutical Sciences, University of Southern California, Los Angeles, California 90089, United States; Department of Chemistry, University of Southern California, Los Angeles, California 90089, United States; Wrigley Institute for Environment and Sustainability, Los Angeles, California 90089, United States; orcid.org/0000-0003-2955-7569; Email: clayw@usc.edu

Travis J. Williams – Department of Chemistry, Donald P. and Katherine B. Loker Hydrocarbon Institute, University of Southern California, Los Angeles, California 90089, United States; Wrigley Institute for Environment and Sustainability, Los Angeles, California 90089, United States; orcid.org/0000-0001-6299-3747; Email: travisw@usc.edu

Author Contributions

All authors have given approval to the final version of the manuscript.

Funding Sources

This study was funded by the National Oceanic and Atmospheric Administration pursuant to Sea Grant award (NA24OARX417C0413-T1-01); the National Institute of Health (R21-AI156320); the National Science Foundation (CMMI-2134658, 2227649); the University of Southern California (Dornsife College faculty working group, Zumberge fund, and President's Sustainability Initiative, MC Gill Composites Center); the USC Wrigley Institute for Environmental Studies (Innovation award); and the University of Kansas Endowment (Irving S. Johnson Fund). We thank the NSF (CHE-2018740, DBI-0821671, CHE-

0840366), the NIH (S10 RR25432), and USC Research and Innovation Instrumentation Awards for analytical tools. Wrigley Fellowship support to C. O. is gratefully acknowledged. We thank the Advanced Composite Technology Center (ACTC), China, for post-consumer composite samples.

Notes

The authors declare no competing financial interest.

ACKNOWLEDGMENT

We thank Tom Czyszczon-Burton for help with XPS experiments, Cesar Reyes for help with obtaining IR spectra, Qixuan Chang for obtaining SEM imaging and Shauna Moore for technical assistance in *A. nidulans* strain construction. We also thank Y. Justin Lim for useful discussions. Biological scheme was created with BioRender.com

ABBREVIATIONS

CFRP, carbon fiber reinforced polymer; OTA, (2Z,4Z,6E)-octa-2,4,6-trienoic acid; *A. nidulans, Aspergillus nidulans*; PKS, polyketide synthase; HPLC-DAD, high performance liquid chromatography with diode-array detection; MM, minimal media; GMM, glucose minimal media; LMM, lactose minimal media; BAMM, benzoic acid minimal media; rCF, recovered carbon fiber.

REFERENCES

1. Liu, T., Shao, L., Zhao, B., Chang, Y.-C. & Zhang, J. Progress in Chemical Recycling of Carbon Fiber Reinforced Epoxy Composites. *Macromol. Rapid Commun.* **2022**, *43*, 2200538.
2. Ma, Y. & Nutt, S. Chemical Treatment for Recycling of Amine/Epoxy Composites at Atmospheric Pressure. *Polym. Degrad. Stab.* **2018**, *153*, 307–317.
3. Kumar, S. & Krishnan, S. Recycling of Carbon Fiber with Epoxy Composites by Chemical Recycling for Future Perspective : a Review. *Chem. Pap.* **2022**, *74*, 3785–3807.
4. Wu, Z. *et al.* Interfacially Reinforced Unsaturated Polyester Carbon Fiber Composites with a Vinyl Ester-Carbon Nanotubes Sizing Agent. *Compos. Sci. Technol.* **2018**, 164, 195–203.
5. Jiang, D. *et al.* Reinforced Unsaturated Polyester Composites by Chemically Grafting Amino-POSS Onto Carbon Fibers with Active Double Spiral Structural Spiralphosphodicholor. *Compos. Sci. Technol.* **2014**, *100*, 158–165.
6. Wonderly, C.; Grenestedt, J.; Fernlund, G.; Cepus, E. Comparison of Mechanical Properties of Glass Fiber/Vinyl Ester and Carbon Fiber/Vinyl Ester Composites. *Compos. Part B* **2005**, *36*, 417–426.
7. Mohsen, S. *et al.* Fire-Retardant Unsaturated Polyester Thermosets: The State-of-the-Art, Challenges and Opportunities. *Chem. Eng. J.* **2022**, *430*, 132785.
8. Wu, Y.; Fei, M.; Qiu, R.; Liu, W.; Qui, J. A Review on Styrene Substitutes in Thermosets and Their Composites. *Polymers (Basel).* **2019**, *11*, 1815.
9. Navarro, C. A. *et al.* A Structural Chemistry Look at Composites Recycling. *Mater. Horizons* **2020**, *7*, 2479–2486.
10. Torkaman, N. F.; Bremser, W.; Wilhelm, R. Catalytic Recycling of Thermoset Carbon Fiber-Reinforced Polymers. *ACS Stain. Chem. Eng.* **2024**, *12*, 7668–7682.
11. Akbar, A.; Liew, K. M. Assessing Recycling Potential of Carbon Fiber Reinforced Plastic Waste in Production of Eco-Efficient Cement-Based Materials. *J. Clean. Prod.* **2020**, *274*, 123001.
12. Navarro, C. A. *et al.* Catalytic, Aerobic Depolymerization of Epoxy Thermoset Composites. *Green Chem.* **2021**, *23*, 6356–6360.
13. Cerruti, P. *et al.* Up-Cycling End-of-Use Materials: Highly Filled Thermoplastic Composites Obtained by Loading Waste Carbon Fiber Composite into Fluidified Recycled Polystyrene. *Polym. Compos.* **2014**, *35*, 1621–1628.
14. Chakraborty, I. *et al.* Massive Electrical Conductivity Enhancement of Multilayer Graphene/Polystyrene Composites Using a Nonconductive Filler. *ACS Appl. Mater. Interfaces* **2014**, *6*, 16472–16475.
15. Qi, X.-Y. *et al.* Enhanced Electrical Conductivity in Polystyrene Nanocomposites at Ultra-Low Graphene Content. *ACS Appl. Mater. Interfaces* **2011**, *3*, 3130–3133.
16. Sriprom, W.; Sirivallop, A.; Choodum, A.; Limsakul, W.; Wongniramaiku, W. Plastic/Natural Fiber Composite Based on Recycled Expanded Polystyrene Foam Waste. *Polymers (Basel).* **2022**, *14*, 2241.
17. Ballner, D. *et al.* Lignocellulose Nanofiber-Reinforced Polystyrene Produced from Composite Microspheres Obtained in Suspension Polymerization Shows Superior Mechanical Performance. *ACS Appl. Mater. Interfaces* **2016**, *8*, 13520–13525.
18. Partenheimer, W. Valuable Oxygenates by Aerobic Oxidation of Polymers Using Metal /Bromide Homogeneous Catalysts. *Catal. Today* **2003**, *81*, 117–135.
19. Das, M.; Chacko, R.; Varughese, S. An Efficient Method of Recycling of CFRP Waste Using Peracetic Acid. *ACS Sustainable Chem. Eng.* **2018**, *6*, 1564–1571.
20. Ahrens, A. *et al.* Catalytic Disconnection of C–O bonds in Epoxy Resins and Composites. *Nat.* **2023**, *617*, 730–737.
21. Sullivan, K. P. *et al.* Mixed Plastics Waste Valorization Through Tandem Chemical Oxidation and Biological Funneling. *Science* **2022**, *211*, 207–211.
22. Rabot, C. *et al.* Polystyrene Upcycling into Fungal Natural Products and a Biocontrol Agent. *J. Am. Chem. Soc.* **2023**, *145*, 5222–5230.
23. Xiao, C.; Zhang, L.; Hao, H.; Wang, W. High Selective Oxidation of Benzyl Alcohol to Benzylaldehyde and Benzoic Acid with Surface Oxygen Vacancies on W18O49/Holey Ultrathin g-C_3N_4 Nanosheets. *ACS Stain. Chem. Eng.* **2019**, *7*, 7268–7276.
24. Lee, D.-S. *et al.* Asperlin From the Marine-Derived Fungus Aspergillus sp. SF-5044 Exerts Anti-inflammatory Effects Through Heme Oxygenase-1 Expression in Murine Macrophages. *J. Pharmacol. Sci.* **2011**, *116*, 283–295.
25. Grau, M. F. *et al.* Hybrid Transcription Factor Engineering Activates the Silent Secondary Metabolite Gene Cluster for (+)-Asperlin in Aspergillus nidulans. *ACS Chem. Biol.* **2018**, *13*, 3193−3205.
26. Messiha, H. L.; Payne, K. A. P.; Scrutton, N. S.; Leys, D. A Biological Route to Conjugated Alkenes: Microbial Production of Hepta-1,3,5-triene. *ACS Synth. Biol.* **2021**, *10*, 228–23.
27. Martins, T. M. *et al.* The Old 3-Oxoadipate Pathway Revisited : New Insights in the Catabolism of Aromatics in the Saprophytic Fungus Aspergillus nidulans. *FUNGAL Genet. Biol.* **2015**, *74*, 32–44.
28. Antunes, M. S.; Hodges, T. K.; Carpita, N. C. A Benzoate-Activated Promoter from Aspergillus niger and Regulation of its Activity. *Appl. Microbiol. Biotechnol.* **2016**, *100*, 5479–5489.
29. Sahasrabudhe, S. R. & Modi, V. V. Hydroxylation of Benzoate and its Chlorinated Derivatives in Aspergillus niger. *Biochem. Int.* **1985**, *10*, 525–529.

Supplementary Information

Composite Recycling with Biocatalytic Thermoset Reforming

Clarissa Olivar,[‡,§] Zehan Yu,[#] Ben Miller,[‡,v] Maria Tangalos,[‡,v] Cory B. Jenkinson,[‖] Steven R. Nutt,[#] Berl R. Oakley,[‖] Clay C.C. Wang,[‡,v,*] Travis J. Williams[‡,*]

[‡]Department of Chemistry, Donald P. and Katherine B. Loker Hydrocarbon Institute, and Wrigley Institute for Environment and Sustainability, University of Southern California, Los Angeles, California 90089, United States

[#]Department of Chemical Engineering & Materials Science and M.C. Gill Composites Center, University of Southern California, Los Angeles, California 90089, United States

[v]Department of Pharmacology & Pharmaceutical Sciences, University of Southern California, Los Angeles, California 90089, United States

[‖]Department of Molecular Biosciences, University of Kansas, Lawrence, Kansas 66045, United States

*Corresponding author emails: travisw@usc.edu, clayw@usc.edu

Contents

1. General Information

Materials

Acetone, chloroform, ethyl acetate, dimethyl sulfoxide, *n*-hexane, methanol, hydrogen peroxide, and D-lactose monohydrate were purchased commercially from VWR. Benzyl alcohol and *N*-hydroxyphthalimide (NHPI) were purchased commercially from Ambeed. Acetic acid, hydrochloric acid, sulfuric acid, nitric acid, and benzoic acid were purchased commercially from Sigma Aldrich. Tripotassium phosphate trihydrate was purchased commercially from Oakwood Chemical. Manganese nitrate tetrahydrate was purchased commercially from Beantown Chemical. Cobalt nitrate hexahydrate was purchased commercially from Thermo Fisher Scientific. Acetic acid-d_4 and methanol-d_4 were purchased from Cambridge Isotopes Laboratories. D-glucose was purchased commercially from Criterion. All chemicals were used as received, without any further purification.

Characterization methods

^{1}H and ^{13}C{^{1}H} NMR spectra were obtained by a Varian VNMRS 400 or 600 spectrometer at room temperature and processed via Mestrelab Mnova. All the chemical shifts are shown in units of ppm. ^{1}H NMR data recorded in acetic acid-d_4 and methanol-d_4 are referenced to residual internal CH_3COOD (δ 2.04) and CH_3OD (δ 3.31), respectively. ^{13}C{^{1}H} NMR data recorded in methanol-d_4 is referenced to residual internal CH_3OD (δ 49.15).

HPLC-DAD (analytical) spectra for OTA quantification were acquired using an Agilent 1260 Infinity II mass spectrometer equipped with a reverse phase C18 column (Phenomenex kinetex EVO C18 Column; particle size, 5 μm; column, 4.6 mm x 150 mm) with a flow rate of 1 mL min^{-1}. The solvents used were 100% double distilled water (solvent A) and 100% acetonitrile (solvent B), each supplemented with 0.05% trifluoroacetic acid. The solvent gradient used was 0% to 60% solvent B from 0 to 23 min, 60% to 100% solvent B from 23 to 24 min, 100% solvent B from 24 to 25 min, 100% to 0% solvent B from 25 to 26 min, and re-equilibration with 0% solvent B from 26 to 35 min. The OTA peak occurred at 16.8 minutes. A UV lamp of wavelength 300 nm was used, with peak width > 0.1 min, 2 s response time, 2.5 Hz.

Preparative HPLC-DAD for OTA purification was completed using an Agilent 1260 Infinity II mass spectrometer equipped with a reverse phase C18 column (COSMOSIL Packed Column 5C18-AR-II; particle size, 5 μm; column, 1.0 mm ID x 250 mm) with a flow rate of 8 mL min^{-1}. The solvents used were 100% double distilled water (solvent A) and 100% acetonitrile (solvent B), each supplemented with 0.05% trifluoroacetic acid. The solvent gradient used was: 34% solvent B from 0 to 42 min, 34% to 100% solvent B from 42 to 43 min, 100% solvent B from 43 to 58 min, 100% to 34% solvent B from 58 to 59 min, and re-equilibration with 34% solvent B from 59 to 74 min. The OTA peak occurred between 30-35 minutes.

2. Media Recipes and Fungal Metabolism

Media recipes

All media were based on minimal medium (MM): 12.0 g/L $NaNO_3$, 3.04 g/L KH_2PO_4, 1.04 g/L KCl, 1.04 g/L $MgSO_4 \cdot 7H_2O$, 1 ml/L 5.5 M KOH, and 1 ml/L of Hutner's trace elements solution.[1] Glucose minimal medium (GMM) contains MM with the addition of 10 g/L of D-glucose. Lactose minimal medium (LMM) is MM with the addition of 15 g/L of D-lactose. Benzoic acid minimal medium (commercial BAMM) contains MM and 10 g/L of commercially available benzoic acid. Pre- and post-consumer composite minimal media, pre-consumer BAMM and post-consumer BAMM, respectively, contain MM and 10 g/L of benzoic acid isolated from their respective composite digests. After adding the benzoic acid substrate, the commercial BAMM, pre-consumer BAMM, and post-consumer BAMM media were adjusted to pH 8 using additional 5.5 M KOH.

Construction of LO11055

Our starting strain was LO7195 which carries *pyrG89*, *riboB2*, and *pyroA4* along with a deletion of *nkuA* and deletions of the following biosynthetic gene clusters (BGCs): sterigmatocystin BGC [genes AN7804-AN7825 using the AspGD, FungiDB gene designations (FungiDB.org) or *stcA-stcW* plus *aflR* using the gene symbols assigned by Brown et al.,[2]] the emericellamide BGC (AN2545-AN2549; *easA-easD*)[3] and the asperfuranone BGC (AN1029-AN1036; *afoA-afoG*).[4] In a co-transformation, we replaced the promoter of AN11191 (*alnA*) with the promoter of *afoE* (AN1034) using *AfriboB* as a selectable marker, and we replaced the promoter of AN11199 (*alnB*) with the promoter of *afoG* (AN1036) using *AfpyroA* as a selectable marker. The resulting strain was designated LO8952. Next, we replaced the *wA* locus with the *gpdA* promoter driving the *afoA* (AN1029) coding sequence using *AtpyrG* as a selectable marker, creating strain LO8993. In this strain we replaced the *yA* locus with the *afoE* promoter driving *afoA* using the pyrithiamine resistance gene, *ptrA,* as a selectable marker This strain was designated LO9955. LO9955 has no remaining selectable markers, so we deleted the *AtpyrG* gene at the *wA* locus by transforming with a fragment that contained *wA* flanking DNA as well as the *gpdA* promoter and the first kb of the *afoA* coding sequence. Integration of the transforming fragment by homologous recombination evicted the *AtpyrG* gene resulting in pyr^- transformants that were selected on 5-fluoroorotic acid. We designated the resulting strain LO10441. Finally, we replaced the *gpdA* promoter driving *afoA* at the *wA* locus with a 1643 bp sequence containing the AN11489 (metallothionein, *mtnA*) promoter using *AtpyrG* as a selectable marker. The resulting strain was designated LO11055. All transforming constructs were created by fusion PCR[5] and all strains were confirmed by extensive diagnostic PCR.

In LO11055 the *mtnA* promoter drives strong constitutive expression of *afoA* mRNA which is translated into the transcription factor AfoA. AfoA drives expression of *alnA* and *alnB* resulting in OTA production. AfoA also drives expression of the copy of the *afoA* coding sequence that is under control of the afoE promoter resulting in additional production of AfoA. The resulting high levels of AfoA drive additional expression of *alnA* and *alnB*, resulting in strong constitutive OTA production.

Sequence of the AN11489 (mtnA) promoter (1646 bases including the ATG start codon for afoA)

CTTCAATTCTCAACAGTAGACCCGTTAGTTCCTTCTCGGTGTATACTCGGCGC
ACGACTCGGTGGTCTGATCCCACTTGTTTATCAATCAGCGCCAAACAAAGCAGTAGC

CACCGCTCTAATCCGCATTAATCCTCCAAGACTTCTCCCACGCAGTAGGCTAGTCTA
TCAGTTAGTCAGATCCATCATCGTATCTCCGATCATCGCTTGCGGCTGTCGCGGGTTT
CCAAGAGCAGAGCAGTGGGCACTGCGCCATTATCGCTAATGCAGGAAATACTTCAT
AGCTCCATCCTACCCCACAATGGCCAGGGCACCAGTTGCACCTGAAACTTCATTGTG
GTGCCCAGGACCCTTCTTGGGCTCTGAGGCATTTTCGCCTTTCGCATTTGAGTATGGA
TACCGATGATACCGCCAAGACAAGAGTCTGTGAGCTGCGCGGGATGATAAGGCTTT
GAGAAACAGGTCGCAAAGATGGAAATGCCTGAGCTCAAGCTTCCGAGATCGACTCC
AGATGACCGTGTCCGGTGCTGGTCATGGCAAGGCATTCTCACCAATAGTATCAATCC
AGGAAACTACTCTGTTCAAGGACTGGAGATAAGATGGTGCCCCGTGCAGCAACAAA
GCATACGGGGCGACGTTAGAGCGCTTGCTTACCTTGCTCAGGACTCCCAACCAAACA
CCGAATGCAACTAGCAGTGCTCCCCACTTAAGTAATAGGATATCGTAAATACTGGGT
CGCAAGAAACCATCTTCTTATTGCTAGCCTTACTTTCGGGCTTTACGTATGGGGCTTT
GAACTATGCAGTATGGAGGAACGTGGCATGACATGGACCTATACAGCATTCGGGCT
TCCTCTGCATGAAGATCGGAGGAGAGCTTGGTCTCTTTCGACGGAAAGGAAGATCTT
GCTGCTTTCCTCTTGATTCAGAATCGTTTAACCTGGACATCATATCGCATCTGCATGC
AATAACCCAGGCACCTGAACCCCCACATCTTACCACGCCGAGGCATTCATACAACCT
TCCAGCAGTGAGCCCCTCCCTCCTGGACTACACCAACAGTGATATAGACACGGCGTT
AAGTTTCAGCATGACCTGGTTTTGGCTTGATCGGCAAATCGTAGCAGGGCGTCAAAG
AAAACAAATCGGATGGTAACTGGGGCCTTGCTGTTGTTGCTATTGGGGGACGTCTTG
CCCGCCAACACACCACCCACACCTGCTGCACCACATGGATTCTTGCAGACTGTTCGG
TGTCCACTATGCTCCACTGCCAGACGCAGTATGCTGAGCCTGTCCAGTCAGAGCACC
AAGGGTAAGCTGCGTAGGTCGTAACCGTGCATGTGCAGGCTGCAATATCGGCGGTT
GTAGGCGTGGGCGTGGGCGTGGGCGTGGGTGAAAGAAGGCTGCCATACTGAGGTGA
AGTCAGTGTCAGATGTAACAGGCGTACTCTTAGTGAGGGGAACTAGTGTAAGGTAG
CAATCCTAGTCCAGGATAGCCAGGAAGAAGAGATATATAAGGAGCCTCGTCCCCAA
GGTTCTCTTCTCTTCCCTATCCATCTGCATCCTATCGCGACTTCCTCATCCAATCAAT
CAACCAACCAACCAACCATCTTCCACCGGTTTATCTACCAACAAACACCATCAACAT
G

Culturing LO11055 and generating a (2Z,4Z,6E)-octa-2,4,6-trienoic acid (OTA) standard

In four 1 L Erlenmeyer flasks, 2.5 x 10^8 spores were inoculated into 250 mL of GMM. The cultures were incubated in the dark for 5 days at 37 °C with shaking of 150 rpm. After the 5-day incubation, cultures were removed from the incubator and filtered *in vacuo* to separate the mycelia from the media. The media were placed on ice and the pH was adjusted to ca. 3 using 6 M HCl. The media were then extracted three times with equal portions of ethyl acetate (1 L) and the solvent was subsequently dried *in vacuo* to reveal a light brown solid. This crude media extract underwent preparative HPLC-DAD according to the aforementioned conditions to isolate OTA. The purified HPLC fractions were dried *in vacuo* resulting in a white crystalline solid. The dry OTA sample was confirmed via ^{1}H NMR (Figure S23 and Table S11), ^{13}C NMR (Figure S24 and Table S12), high resolution mass spectrometry analysis (ESI/QTOF), m/z = 137.061 ([M]$^-$ calc for $C_8H_{10}O_2$ = 138.068). This purified OTA was used to prepare the standard curve for quantification. The sample was stored in the dark at 4 °C to prevent degradation.

Culturing LO11055 for (2Z,4Z,6E)-octa-2,4,6-trienoic acid (OTA) yield comparison

In a 25 mL Erlenmeyer flask, 1.0 x 10^7 spores were inoculated into 10 mL of either MM, GMM, LMM, commercial BAMM, pre-consumer BAMM, or post-consumer BAMM. Each

condition was completed in triplicate for proper statistical analysis. The cultures were incubated in the dark for 5 days at 37 °C with shaking at 150 rpm.

Extraction and quantification of (2Z,4Z,6E)-octa-2,4,6-trienoic acid (OTA)

After the 5-day incubation, cultures were removed from the incubator and gravity filtered to separate the mycelia from the media. For each respective culture, the medium was placed in a 50 mL falcon tube on ice and the pH was adjusted to ca. 3 using 6 M HCl. The media were extracted three times with equal portions of ethyl acetate to media (10 mL) and the solvent was subsequently dried (TurboVap LV). To retrieve any intracellular OTA, mycelia were simultaneously lysed and extracted by vortexing the mycelia in 10 mL of ethyl acetate in a 15 mL falcon tube. The mycelia were extracted once, gravity filtered to remove the hyphal mass, and the resulting extract was dried (TurboVap LV). Medium and mycelia extracts were combined for each respective culture. Samples were redissolved in 10 mL methanol and the yield was determined via analytical HPLC-DAD (R^2 = 0.9985) according to the aforementioned method with a sample injection volume of 10 µL. Linear regression was completed using Microsoft Excel ver. 16.87, and modeling of data and statistical analysis of data was completed using MATLAB ver. 2024a.

3. Synthetic Procedure

General procedure for the pretreatment of pre- and post-consumer carbon fiber reinforced polymers (CFRPs)

CFRP (38.1 x 25.4 mm, 4.0981 g, FiberGlast Part #78 – Laminating Resin AropolTM L 67355 T-20 TS, FiberGlast Part #77 Polyester Molding Resin, or post-consumer), benzyl alcohol (100 mL), and tripotassium phosphate trihydrate (0.540 g, 1.98 mmol) were placed in a 500 mL four neck reaction kettle round bottom flask equipped with a reflux condenser and stir bar and heated to 180 ºC for 24 hours under nitrogen. The reaction was removed from heat and allowed to cool to room temperature. The benzyl alcohol solution was filtered *in vacuo* to collect a heterogeneous solid and a clear yellow filtrate. The filtered solid was washed with acetone and dried *in vacuo*. The carbon fiber plies were washed with acetone, dried with a paper towel, and residual solvent was allowed to evaporate in air overnight.

Determination of residual benzyl alcohol content

CFRP (25.4 mm x 50.8 mm, 1.9844, Fiber Glast Part #77 Polyester Molding Resin), benzyl alcohol (100 mL), and tripotassium phosphate trihydrate (0.230 g, 0.86 mmol) were placed in a 500 mL four neck reaction kettle round bottom flask equipped with a reflux condenser and stir bar and heated to 180 ºC for 24 hours under nitrogen. The reaction was removed from heat and allowed to cool to room temperature. The benzyl alcohol solution was filtered *in vacuo* to collect a heterogeneous solid and a clear yellow filtrate. The filtered solid and fibers were washed with deionized water and acetone. Residual solvent was allowed to evaporate overnight before weighing (37.6779 g) components in an oven dried petri dish. The petri dish and its components were dried in an oven for a week before reweighing (37.6451 g). Benzyl alcohol removed (33 mg).

General procedure for the digestion of pretreated pre-consumer (Fiber Glast Part #77 Polyester Molding Resin) CFRPs

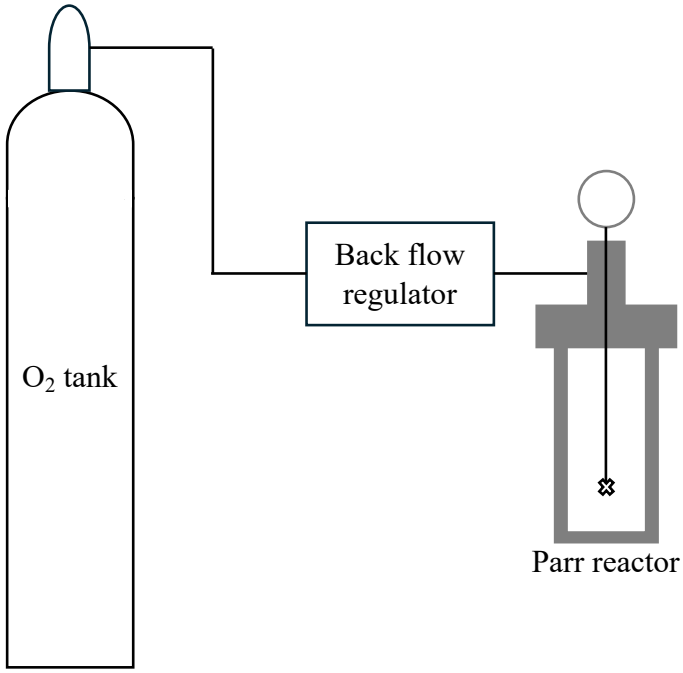

Figure S1. Apparatus setup to enable continuous oxygen delivery to the Parr reactor.

The pretreated carbon fiber plies and the resulting solid were added to a 500 mL Parr reactor (Figure S1) along with manganese nitrate tetrahydrate (0.290 g, 1.16 mmol), cobalt nitrate hexahydrate (0.297 g, 1.02 mmol), *N*-hydroxyphthalimide (0.294 g, 1.80 mmol), and acetic acid (100 mL). The reactor was closed, sparged with O_2 three times, filled with 3.4 atm O_2, and heated to 150 ºC. Once the reaction reached 150 ºC, the pressure on the oxygen tank was increased to 6.1 atm to ensure continuous flow of oxygen into the system. The reaction proceeded for 24 hours while stirring. The reactor was allowed to cool to room temperature before collecting the solution and the carbon fiber plies. The resulting mixture was purified via the procedure outlined below. Isolated benzoic acid: 1.177 g (yield: 93-102%) ^{1}H NMR (acetic acid-d_4, 600 MHz): δ (ppm) 7.49 (t, 2H), 7.63 (t, 1H), 8.09 (d, 2H).

General procedure for the digestion of pretreated pre-consumer (Fiber Glast Part #78 – Laminating Resin AropolTM L 67355 T-20 TS) CFRPs

The pretreated carbon fiber plies and the resulting solid were added to a 500 mL Parr reactor (Figure S1) along with manganese nitrate tetrahydrate (0.268 g, 1.07 mmol), cobalt nitrate hexahydrate (0.287 g, 0.99 mmol), *N*-hydroxyphthalimide (0.261 g, 1.60 mmol), and acetic acid (300 mL). The reactor was closed, sparged with O_2 three times, filled with 3.4 atm O_2 and heated to 150 ºC. Once the reaction reached 150 ºC, the pressure on the oxygen tank was increased to 6.1 atm to ensure continuous flow of oxygen into the system. The reaction proceeded for 24 hours while stirring. The reactor was allowed to cool to room temperature before collecting the solution and the carbon fiber plies. The mixture was purified via the procedure outlined below. Isolated benzoic acid: 0.401 g (yield: 37-42%).

General procedure for the digestion of pretreated post-consumer CFRPs

The pretreated carbon fiber plies and the resulting solid were added to a 500 mL Parr reactor (Figure S1) along with manganese nitrate tetrahydrate (0.543 g, 2.16 mmol), cobalt nitrate hexahydrate (0.546 g, 1.88 mmol), *N*-hydroxyphthalimide (0.556 g, 3.41 mmol), and acetic acid (300 mL). The reactor was closed, sparged with O_2 three times, filled with 3.4 atm O_2 and heated to 150 ºC. Once the reaction reached 150 ºC, the pressure on the oxygen tank was increased to 6.1 atm to ensure continuous flow of oxygen into the system. The reaction proceeded for 24 hours while stirring. The reactor was allowed to cool to room temperature before collecting the solution and the carbon fiber plies. The mixture was purified via the procedure outlined below. Isolated benzoic acid: 0.217 g (yield: 16-25%).

General procedure for carbon fiber purification

The four obtained carbon fiber plies were washed with acetic acid and ethyl acetate. One of the plies was soaked in diluted HCl (pH 5) for one hour, washed with DI water (150 mL), sonicated in DI water for 5 minutes, rinsed with acetone, and allowed to dry in air. The remaining three plies were sonicated in HPLC grade water for 5 minutes. One of the three plies was washed with acetone and allowed to dry in air. The remaining two plies were soaked in diluted HNO_3 of varying pHs (pH 2 and pH 5) for one hour. Both plies were washed with HPLC grade water (150 mL), rinsed with acetone, and allowed to dry in air. The fibers were imaged via SEM (Figures S3-S7).

General procedure for carbon fiber resizing via nitric acid digestion[6,7]

Loose carbon fibers recovered after the two-step digestion of pre-consumer CFRPs (FiberGlast Part #77 Polyester Molding Resin) outlined above, were refluxed at 100 ºC in nitric acid for 40 minutes resulting in a clear dark orange solution. Carbon fibers were washed with DI water until pH 7. The fibers were soaked for an additional 15 minutes in DI water and the pH of the water was retested to confirm pH 7. Carbon fibers were dried *in vacuo* at 120 ºC for 2 hours and characterized via XPS (Figure S10).

General procedure for benzoic acid purification from pre-consumer composite digest

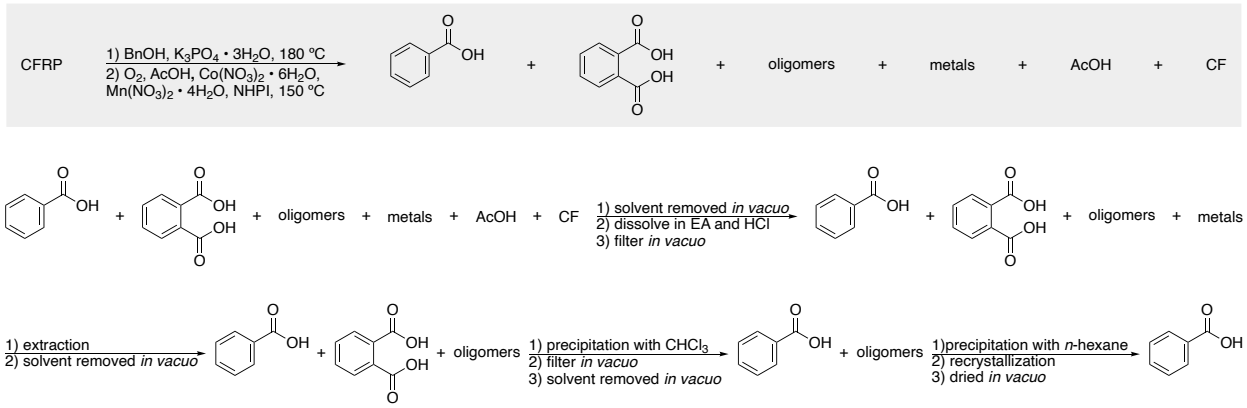

Figure S2. Purification of benzoic acid from composite digest where CFRP: carbon fiber reinforced polymer; CF: carbon fiber; EA: ethyl acetate; HCl: hydrochloric acid diluted in DI water (pH 2); and $CHCl_3$: chloroform.

Solvent was removed from the resulting digest *in vacuo* resulting in a dark brown product. Ethyl acetate and acidic water (HCl, pH 2) were added to the crude product and filtered *in vacuo* to remove lose carbon fibers. An extraction was performed with ethyl acetate and acidic water (HCl, pH 2, 3 x 150 mL). The organic layer was collected, dried over Na_2SO_4, and decanted. Solvent was removed *in vacuo* resulting in a yellow powder. Chloroform was added to the yellow powder and the solution was filtered through celite. Filtrate was collected and solvent was removed *in vacuo* resulting in a yellow powder. *n*-Hexane was added to the yellow powder, stirred for 30 minutes at room temperature, and the solution was filtered *in vacuo* resulting in a clear, off-white filtrate and light-yellow powder. Solvent was removed *in vacuo* affording a shiny off-white solid. Crude benzoic acid was recrystallized in DI water, dissolved in ethyl acetate, and filtered through celite. Solvent was removed *in vacuo* affording a white powder. The product was confirmed via ^{1}H NMR (Figures S15-S16).

4. Composite Manufacturing and Characterization

Manufacturing of pre-consumer carbon fiber reinforced polymer (CFRP) composites

A matrix of 77 and 78 CFRP was formulated using FiberGlast Part #77 Polyester Molding Resin (FiberGlast 77) or FiberGlast Part #78 – Laminating Resin AropolTM L 67355 T-20 TS (FiberGlast 78) with FiberGlast 69 methyl ethyl ketone peroxide hardener. Ninety grams of resin were poured into a mixing cup. The hardener was added to facilitate curing at a ratio of 1% and 1.25% for FiberGlast 77 and FiberGlast 78, respectively. The mixture was stirred for 10 minutes before use. Note that FiberGlast Part #78 was the resumed supply of a substantially similar product following the discontinuation of #77.

A release agent (LOCTITE FREKOTE 770-NC, Henkel) was applied to an aluminum tool plate by wiping it with a cloth. Three coats were applied in total. A layer of pre-cut CF fabrics (203 x 203mm, 2 x 2 twill, FiberGlast 1069) was placed on the coated tool plate. The pre-mixed resin was brushed onto the fabric. After the first layer of fabric was thoroughly wetted, a second layer was plotted on top and compacted by a roller to remove entrapped air. The laminate was built up to four layers of fabric following this procedure. A peel ply and a release film (Airtech, Release Ease 234 TFNP) were placed on the laminate to provide a better surface finish. The laminate was then enclosed in a vacuum bag and compacted by pulling a vacuum.

After lamination, the laminate was cured at room temperature for 24 hours. Fully cured laminates were then cut into 50.8 x 50.8 mm samples on a water-jet cutter (ProtoMax, OMAX).

Resin contents (W_r) for CFRP composites

The resin content of CFRPs (Tables S1-S3) was determined following the method described in ASTM D3171-22 (procedure B). Fully cured FiberGlast 77, FiberGlast 78, and post-consumer panels were cut into 50.8 x 10.2 mm specimens on water-jut cutters (ProtoMax, OMAX). Specimens were cleaned with DI water and dried in a convection oven at 80 °C overnight. Each CFRP was weighed to the nearest thousandths place (M_I) and placed into individual 250 mL two-neck round bottom flasks containing 50 mL of sulfuric acid. The flask was equipped with a reflux condenser and heated to 100 °C in an oil bath. A solution of 30% hydrogen peroxide was added to the mixture in 10 mL aliquots after two, three, and four hours (30 mL total). The reaction was terminated after five hours and allowed to cool to room temperature. Carbon fibers (CFs) were filtered *in vacuo* and washed with DI water and acetone. Recovered CFs were dried in a convection oven at 120 °C for 12 hours and were subsequently allowed to cool to room temperature. Recovered CFs were weighed to the nearest thousandths place (M_f). The resin content was determined using the following equation:

$$W_r = \left(\frac{M_f}{M_I}\right) \times 100$$

Mass of polystyrene in CFRP composites

The mass of styrene (S) in the composite was determined via the following equation:

$$S = mass\ of\ composite \times matrix\ \% \times resin\ \% \times styrene\ \%$$

where matrix % is determined via the procedure outlined above and styrene % is given in Table S5 for each material.

Scanning electron microscopy (SEM)

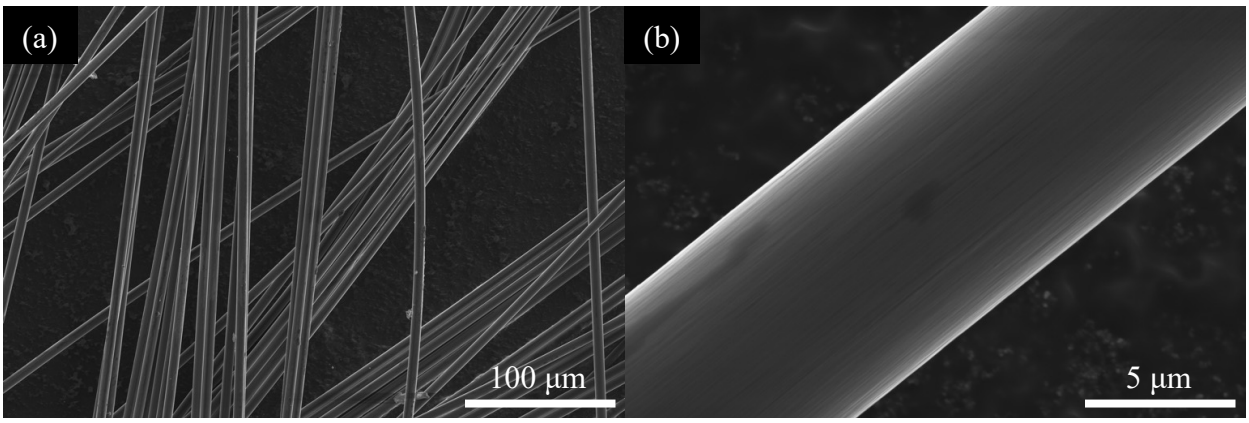

Figure S3. SEM images of virgin carbon fibers at (a) 1,000X and (b) 20,000X.

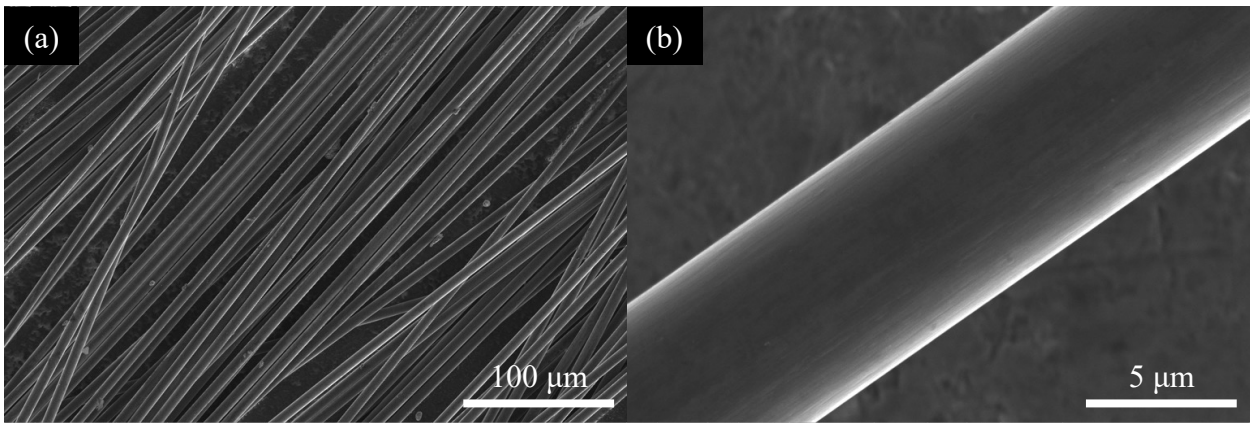

Figure S4. SEM images of rCF washed with H_2O at (a) 1,000X (a) and (b) 20,000X.

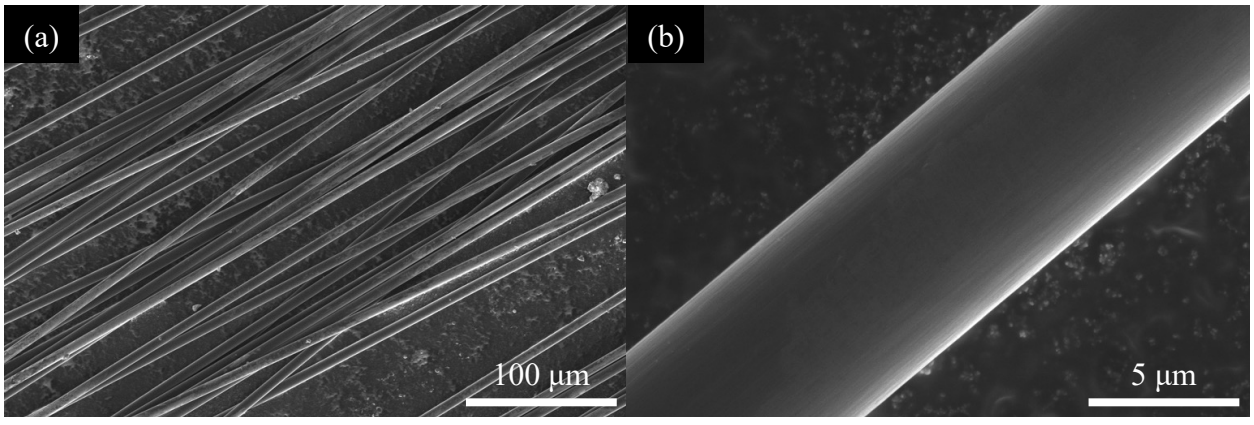

Figure S5. SEM images of rCF washed with HCl pH 5 at (a) 1,000X and (b) 20,000X.

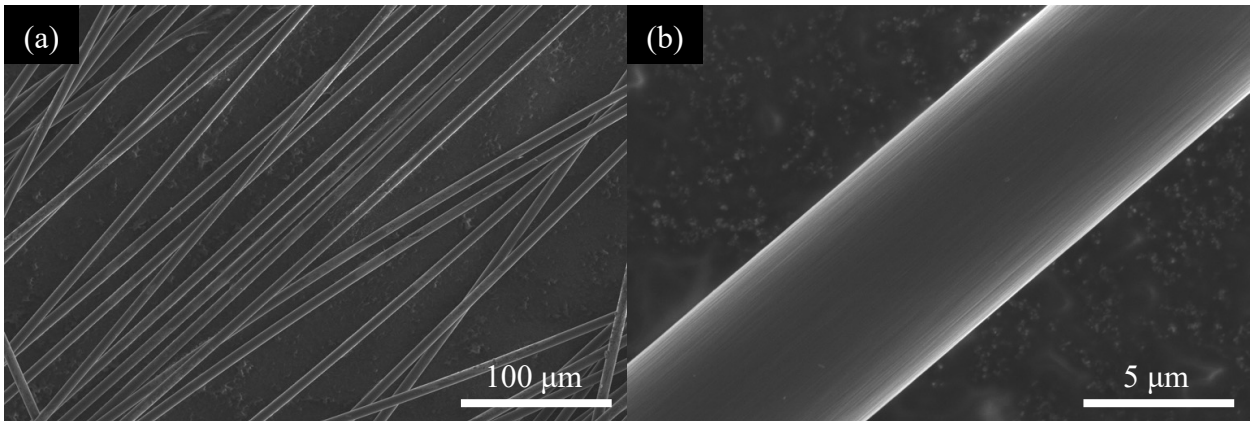

Figure S6. SEM images of rCF washed with HNO_3 pH 5 at (a) 1,000X and (b) 20,000X.

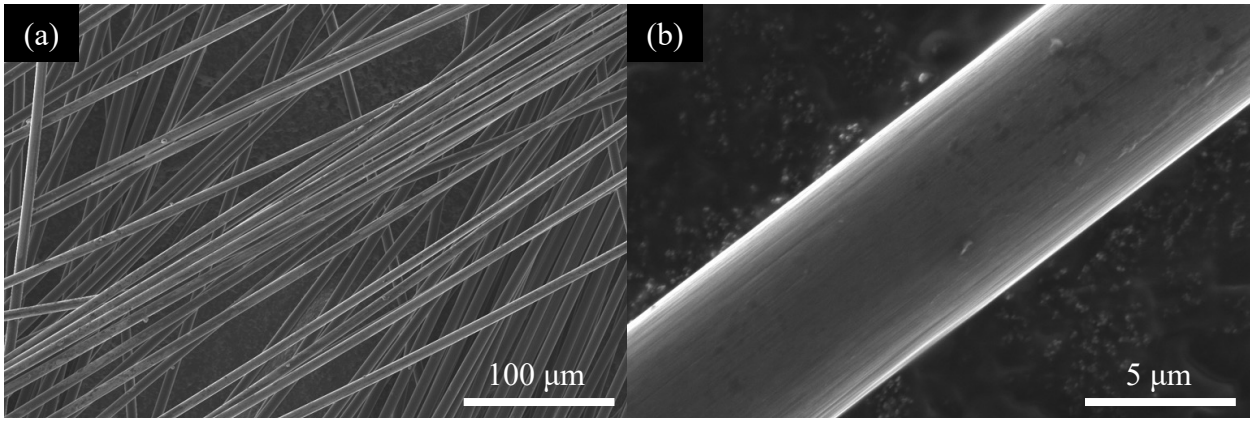

Figure S7. SEM images of rCF washed with HNO_3 pH 2 at (a) 1,000X and (b) 20,000X.

X-ray photoelectron spectroscopy

X-ray photoelectron spectroscopy (XPS, Kratos Axis Ultra DLD) was used to analyze elements and functional groups on the carbon fiber surface. A survey scan (0-1200 ev) was first acquired on each sample, followed by a high-resolution C1s scan. X-ray source was mono aluminum with a 90 ºC incident angle. Curve-fitting of the C1s spectra was performed in CasaXPS software using Shirley baseline and Gaussian-Lorentzian functions, as shown in Figures S8-S10.

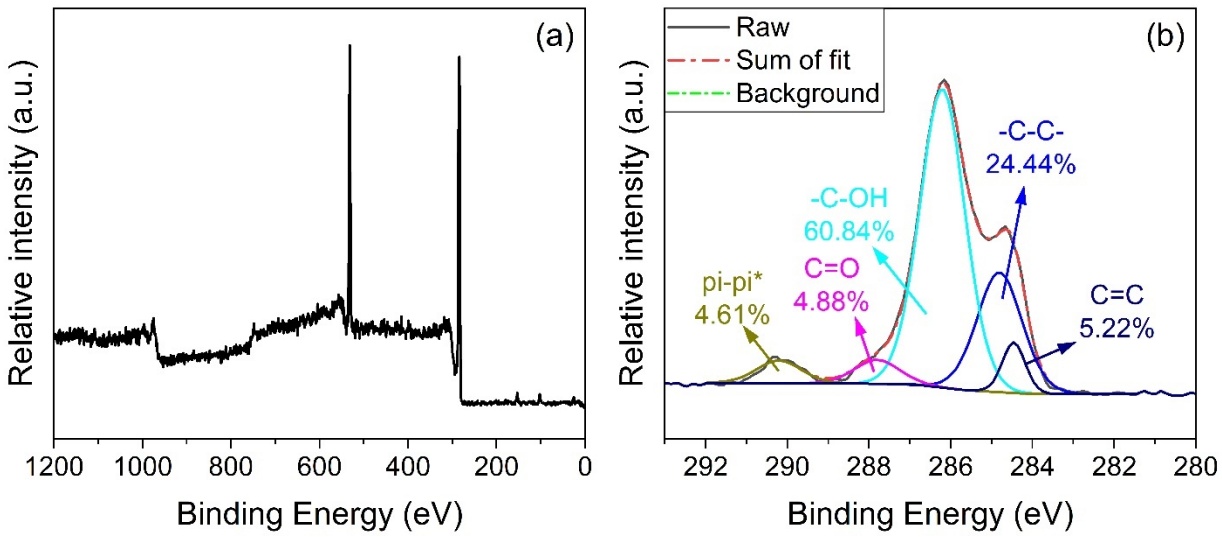

Figure S8. (a) XPS survey and (b) C1S high resolution spectra of virgin carbon fibers.

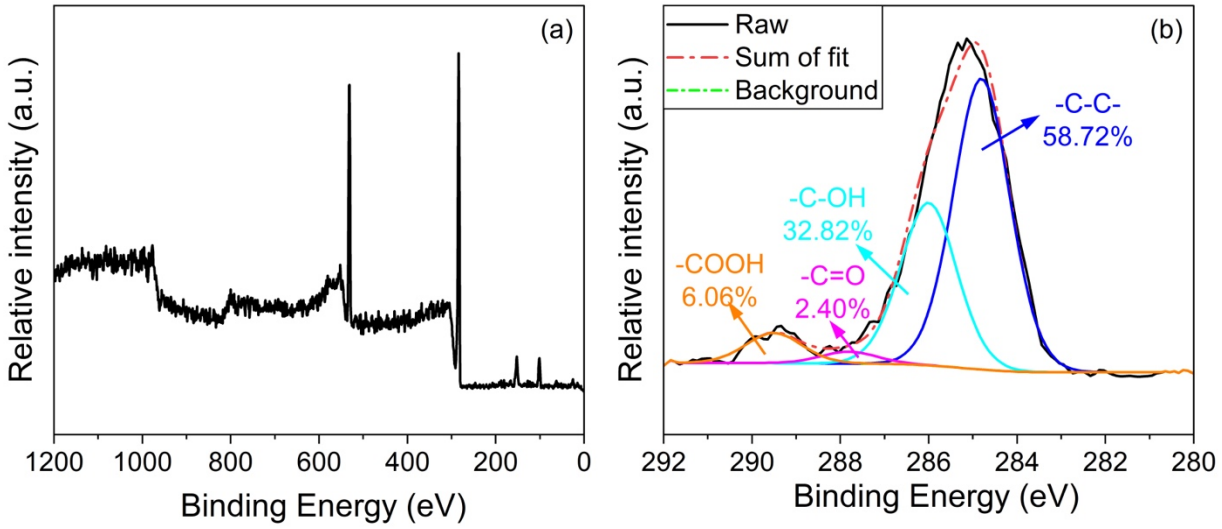

Figure S9. (a) XPS survey and (b) C1S high resolution spectra of recovered carbon fibers.

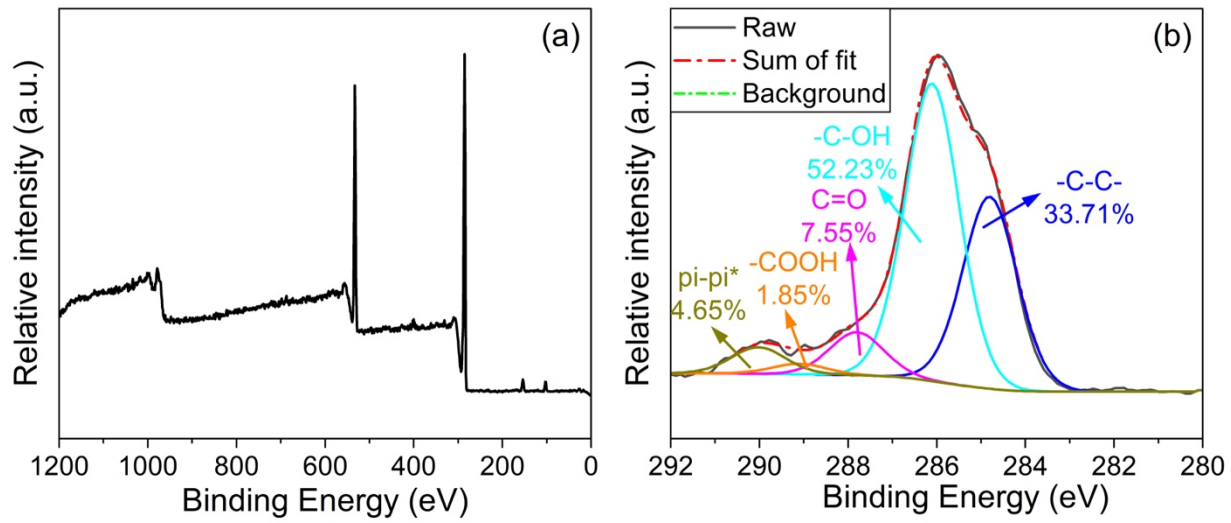

Figure S10. (a) XPS survey and (b) C1S high resolution spectra of recovered carbon fibers treated with nitric acid.

XPS survey spectra show four peaks assigned to C, O, N, and Si. The detailed element compositions of virgin and recovered CFs are summarized in Table S7.

The C1s high-resolution spectra can be curve-fitted into five peaks: C-C (284.8ev), C-OH (286.2 ev), C=O (287.8 ev), O-C=O (288.8 ev) and π-π* satellite (290.2ev).[8] After recycling, C-OH concentration greatly decreased. This indicates that some of the sizing agents of the CFs were removed during recycling. The loss of sizing functionality can be restored by treating recovered CFs in nitric acid as shown in Figure S10.[6,7]

Tensile strength of recovered pre-consumer carbon fibers

The tensile properties of both virgin and recovered CFs were tested in accordance with the ISO 11566 standard. Individual fibers were separated from tows and mounted on paper strips. Paper strips were printed and cut into 81.3 x 25.4 mm, with a 25.4 x 12.7 mm window in the center. Fibers were mount across the center window. Both ends of the fiber were affixed using double sided tape and epoxy adhesive (Henkel E-20HP) to secure the fibers in place.

Once the epoxy adhesive had cured, the mounted samples were examined using a light microscope (Keyence VHX-5000) equipped with a 1500x lens to measure the fiber diameter. The reference length of pixel is calibrated using a reference scale (Keyence OP-87426). The diameter of each sample was measured three times, and the measured values were averaged to obtain the final measurement. The CF cross-sections were assumed to be circular, and the areas were calculated using the averaged diameters.

After mounting the sample onto the load frame, a cut was made in the center of the mounting sheet to free the fiber for testing. The samples were tested at 2mm/min crosshead speed till break. A total of seventy-six tests were conducted, with forty tests performed on virgin carbon fibers and thirty-six tests on recovered CFs, rCFs. The tensile strength was then calculated and plotted against strain (%) using these calculated areas. The slope of stress-strain curves was taken as tensile modulus. Results are summarized in Figure S11 and Tables S8-S10.

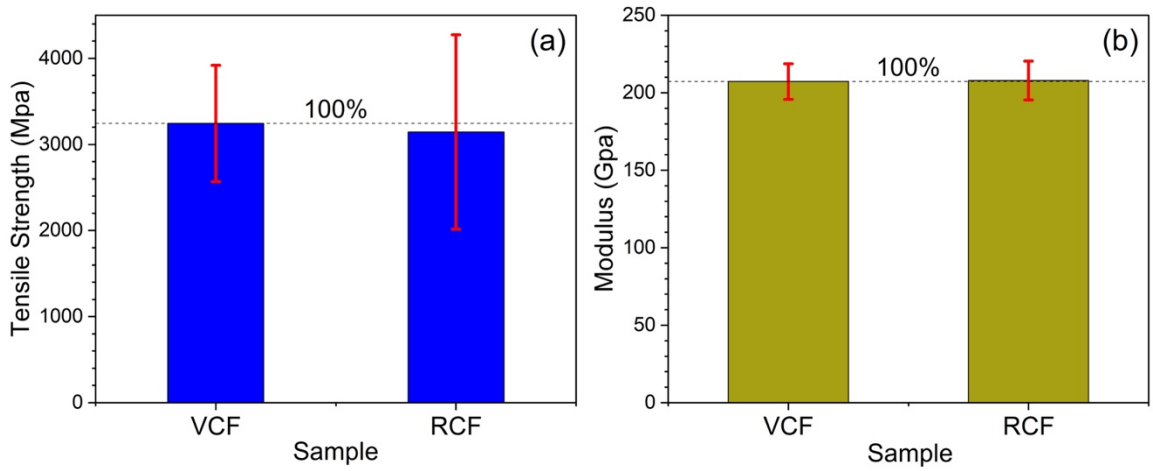

Figure S11. Single fiber tensile test results of virgin carbon fibers, vCF, and recovered carbon fibers, rCF.

Manufacturing of a second-generation composite

Cleaned recovered carbon fiber plies (ca. 50.8 x 50.8 mm) were combined with commercial aerospace-grade resin film, Solvay CYCOM 5320-1, to fabricate prepreg (Figure S12). Resin films were cut into 50.8 x 50.8 mm. One layer of resin film was attached to each side of the recovered fabrics. The stack was then heated and pressed on a hot press (Wabash) at 60 °C with 0.1 tons force for two minutes. After cooling down, release films of prepreg were peeled off, and two additional layers of resin film were attached to the prepreg. The stack was then reheated and repressed on a hot press at 60 °C with 0.1 tons force for an additional two minutes.

Second generation CFRP panels were laminated via the vacuum bag only process using four layers of prepreg. The curing cycle was as follows (1) hold temperature at 60 °C for 2 hours; (2) increase temperature by 1 °C/min until 120 °C is reached; (3) hold temperature at 120 °C for 2 hours; (4) increase temperature by 1.7 °C/min until 177 °C is reached; and (5) hold temperature at 177 °C for 2 hours. A reference 5320-1 CFRP was fabricated following the procedure using virgin CF fabrics (50.8 x 38.1 mm, FiberGlast 1069).

Second generation CFRP cross section

Strips were cut from the second generation CFRP and the reference 5320-1 CFRP using a water-jet cutter (ProtoMax, OMAX). Strips were mounted with transparent resin (CitoPress-1, Struers) for cross-section polishing. Mounted samples were then polished using silicon carbide papers and aluminum oxide slurry. Polished cross-sections were imaged using a light microscope (200X, VHX5000, Kenyence), as shown in Figure S12.

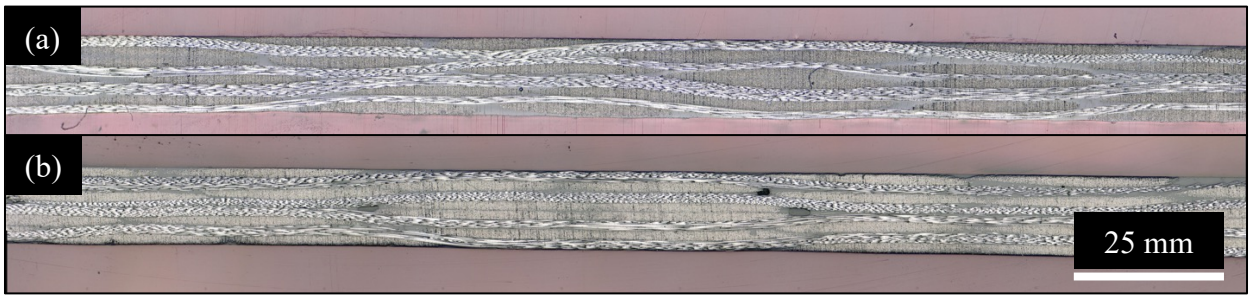

Figure S12. Cross section, at 200X of (a) reference 5320-1 CFRP and (b) second generation CFRP.

5. Supplementary Tables

Table S1. Summary of matrix content weight measurement of FiberGlast Part #77 Polyester Molding Resin CFRP.

Entry	M_I (g)	M_F (g)	W_m (%)
1.	0.6754	0.2464	63.52
2.	0.7222	0.2545	64.76
3.	0.8147	0.2466	69.73
4.	0.8361	0.2511	69.97
5.	0.8383	0.2456	70.70
6.	0.9057	0.2495	72.45
	Average		68.52
	STDEV.P		3.24

Table S2. Summary of matrix content weight measurement of FiberGlast Part #78 – Laminating Resin AropolTM L 67355 T-20 TS CFRP.

Entry	M_I (g)	M_F (g)	W_m (%)
1.	0.8219	0.2592	68.46
2.	0.7016	0.2563	63.47
3.	0.7940	0.2536	68.06
4.	0.6406	0.2564	59.98
5.	0.6335	0.2579	59.29
	Average		63.85
	STDEV.P		3.87

Table S3. Summary of matrix content weight measurement of post-consumer CFRP.

Entry	M_I (g)	M_F (g)	W_m (%)
1.	1.0012	0.2655	73.48
2.	1.0493	0.3114	70.32
3.	1.0374	0.3050	70.60
	Average		71.47
	STDEV.P		1.43

Table S4. Optimization of reaction conditions for pre-consumer CFRPs (FiberGlast Part #77 Polyester Molding Resin CFRPs) of dimensions 50.8 x 38.1 mm. The following are abbreviated for clarity: K_3PO_4: $K_3PO_4 \bullet 3H_2O$; Co: cobalt nitrate hexahydrate; and Mn: manganese nitrate tetrahydrate. Weight percent is relative to the composite.

Entry	BnOH (mL)	K_3PO_4 (%)	Time (hrs)	Co (%)	Mn (%)	NHPI (%)	AcOH (mL)	Time (hrs)
1.	-	-	-	4	4	7	125	24
2.	100	-	24	9	10	9	100	24
3.	100	11	8	4	4	7	100	24
4.	100	11	24	4	4	7	100	24
5.	100	11	24	4	5	7	250	48
6.	100	11	24	7	8	7	100	24

Table S5. Mass characterization of reaction mixture where rCF: recovered carbon fibers; PA: phthalic acid; and BA: benzoic acid. Pre-consumer composite was comprised of FiberGlast Part #78 – Laminating Resin AropolTM L 67355 T-20 TS *or* FiberGlast Part #77 Polyester Molding Resin. Range is provided for benzoic acid yield in both pre- and post- consumer composites to account for standard deviation in matrix content. The benzoic acid yield range for the post-consumer composite additionally accounts for 20-30% styrene content provided by the manufacturer. *: as provided by the manufacturers.

Composite	Matrix styrene content (wt %)*	rCF (g)	PA (g)	Oligomers (g)	BA (g)	BA yield (%)
Pre-consumer (Resin 77)	42.83	-	0.101	1.051	1.177	93-102
Pre-consumer (Resin 78)	33.25	1.489	0.063	0.761	0.401	37-42
Post-consumer	20-30	1.386	0.164	0.333	0.217	16-25

Table S6. Elemental analysis of recrystallized benzoic acid from pre-consumer CFRP (Fiber Glast Part #77 Polyester Molding Resin).

Element	Theoretical	Pre-consumer
Carbon	68.85	68.02
Hydrogen	4.95	4.73

Table S7. XPS analysis summary of vCF: virgin CFs; rCF: recovered CFs; and nrCF: nitric acid treated recovered CFs. *:with sizing.

	Surface Element (%)					C1s Components (%)					
Sample	C	N	Si	O	O/C	C-C	C-OH	C=O	O-C=O	C=C	π-π*
vCf*	78.86	1.25	3.35	16.55	20.99	24.44	60.84	4.88	N/A	5.22	4.61
rCF	74.53	N/A	8.17	17.30	23.21	58.72	32.82	2.40	6.06	N/A	N/A
nrCF	77.54	0.32	2.79	19.35	24.95	33.71	52.23	7.55	1.85	N/A	4.65

Table S8. Single fiber tensile test summary of virgin CFs (vCFs) and recovered CFs (rCFs).

Sample	Diameter (μm)	Strain at Break (%)	Tensile Strength (MPa)	Modulus (Gpa)
vCFs	7.47 ± 0.13	1.49 ± 0.30	3244.96 ± 676.10	207.28 ± 11.44
rCFs	7.46 ± 0.12	1.48 ± 0.48	3145.46 ± 1128.41	207.88 ± 12.55

Table S9. Single fiber tensile strength test results of virgin CFs.

Test #	Diameter (μm)	Strain at break (%)	Force at break (N)	Strength (Mpa)	Modulus (Gpa)
1.	7.44	1.55	0.1474	3391.05	214.67
2.	7.52	1.80	0.1856	4179.80	217.67
3.	7.50	1.78	0.1732	3918.05	207.57
4.	7.53	1.58	0.1560	3507.47	208.47
5.	7.22	1.66	0.1393	3404.38	193.65
6.	7.48	1.12	0.1092	2484.29	206.74
7.	7.63	1.17	0.1186	2594.73	212.20
8.	7.45	1.90	0.1773	4069.13	209.42
9.	7.50	1.21	0.1188	2687.83	213.47
10.	7.68	1.22	0.1255	2707.95	210.64
11.	7.51	1.56	0.1550	3500.47	217.59
12.	7.61	1.52	0.1487	3271.82	208.97
13.	7.39	1.56	0.1614	3765.06	211.09
14.	7.46	0.80	0.0760	1738.11	199.79
15.	7.36	0.81	0.0989	2328.14	202.64
16.	7.57	1.48	0.1450	3224.23	211.45
17.	7.64	1.69	0.1650	3598.33	208.01
18.	7.44	1.66	0.1450	3336.05	192.33
19.	7.46	1.49	0.1378	3151.25	203.84
20.	7.49	1.05	0.0959	2176.95	197.60
21.	7.68	1.58	0.1534	3310.00	203.66
22.	7.49	1.54	0.1475	3345.22	211.79
23.	7.56	1.59	0.1650	3674.86	224.13
24.	7.03	1.83	0.1466	3777.51	200.82
25.	7.48	1.03	0.0985	2239.98	207.54
26.	7.56	2.01	0.2002	4465.49	219.32
27.	7.43	1.28	0.1064	2455.93	187.05
28.	7.43	1.38	0.1293	2983.21	209.32
29.	7.47	1.61	0.1509	3444.00	208.93
30.	7.39	1.31	0.1068	2492.16	184.99
31.	7.58	1.94	0.1801	3997.02	198.44
32.	7.47	1.45	0.1306	2981.25	197.87
33.	7.07	1.36	0.1433	3652.06	232.83
34.	7.57	0.95	0.0779	1730.63	177.73
35.	7.41	1.88	0.1869	4336.84	228.31
36.	7.48	1.84	0.1691	3847.34	201.90
37.	7.50	1.38	0.1388	3140.59	201.90
38.	7.35	1.60	0.1627	3837.28	217.49
39.	7.33	1.71	0.1672	3963.75	229.31
40.	7.53	1.52	0.1375	3088.06	199.87
Average	7.47	1.49	0.1420	3244.96	207.28
STDV.P	0.13	0.30	0.0294	676.10	11.44

Table S10. Single fiber tensile test results of recovered CFs.

Test #	Diameter (μm)	Strain at Break (%)	Force at break (N)	Strength (Mpa)	Modulus (Gpa)
1	7.52	0.95	0.0816	1837.27	197.40
2	7.45	1.97	0.1892	4343.41	197.24
3	7.37	1.22	0.1102	2583.80	209.78
4	7.80	1.28	0.1471	3079.60	209.78
5	7.36	1.85	0.1727	4062.02	217.21
6	7.70	1.25	0.1225	2634.70	208.11
7	7.72	0.90	0.0822	1755.89	191.58
8	7.23	1.77	0.1578	3848.14	218.43
9	7.56	1.03	0.0907	2021.37	195.84
10	7.45	1.09	0.1038	2380.04	216.98
11	7.48	1.50	0.1362	3100.56	202.81
12	7.46	1.19	0.1036	2371.21	197.38
13	7.45	0.85	0.0721	1656.31	191.64
14	7.46	0.95	0.0786	1799.87	190.11
15	7.31	1.41	0.1302	3105.77	219.94
16	7.29	1.90	0.1702	4082.30	214.79
17	7.58	1.44	0.1361	3017.08	209.70
18	7.38	1.25	0.1127	2632.43	210.20
19	7.46	1.24	0.1126	2578.14	209.08
20	7.47	1.99	0.1690	3860.42	194.63
21	7.46	1.95	0.1873	4288.28	223.25
22	7.42	2.14	0.1936	4480.41	213.64
23	7.40	2.26	0.2263	5260.16	233.71
24	7.56	0.66	0.0643	1432.06	205.64
25	7.43	1.64	0.1401	3230.91	199.43
26	7.54	2.00	0.2061	4621.31	232.37
27	7.50	1.84	0.1727	3910.43	212.99
28	7.41	1.83	0.1773	4114.11	222.60
29	7.40	0.71	0.0568	1321.57	185.92
30	7.41	0.59	0.0498	1155.61	192.99
31	7.46	2.14	0.2144	4908.15	229.16
32	7.65	2.07	0.2049	4461.02	213.10
33	7.50	2.35	0.2209	5006.91	212.79
34	7.28	1.37	0.1040	2496.77	184.24
35	7.48	1.35	0.1210	2756.72	206.06
36	7.31	1.42	0.1275	3041.82	213.27
Average	7.46	1.48	0.1374	3145.46	207.88
STDV.P	0.12	0.48	0.05	1128.41	21.00

Table S11. ^{1}H NMR shifts of (2Z,4Z,6E)-octa-2,4,6-trienoic acid compared to literature values.[9] Literature ^{1}H NMR in $CDCl_3$. Experimental ^{1}H NMR in methanol-d_4. Carboxylic acid signal, –COO*H*, is missing from experimental ^{1}H NMR due to H/D exchange with solvent.

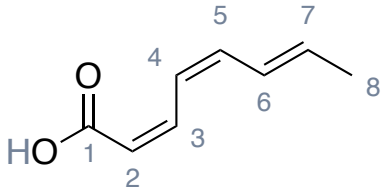

Hydrogen	δ_H (ppm) literature	Splitting	J (Hz)	δ_H (ppm) experimental	Splitting	J (Hz)
1	-	-	-	-	-	-
2	5.67	d	11.3	5.66	d	10.2
3	7.18	dd	11.3, 10.5	7.16	apparent t	11.5
4	7.15	dd	11.1, 10.5	7.10	apparent t	11.4
5	6.36	dd	11.1, 10.5	6.32	apparent t	11.0
6	6.62	dd	14.6, 10.5	6.71	dd	14.8, 11.5
7	5.97	dq	14.6, 6.8	5.98	dq	14.0, 6.9
8	1.85	br d	6.8	1.86	d	6.9
–COO*H*	10.87	br s	-	-	-	-

Table S12. $^{13}C\{^{1}H\}$ NMR shifts of (2Z,4Z,6E)-octa-2,4,6-trienoic acid compared to literature values. [9] Literature $^{13}C\{^{1}H\}$ NMR in $CDCl_3$. Experimental $^{13}C\{^{1}H\}$ NMR in methanol-d_4.

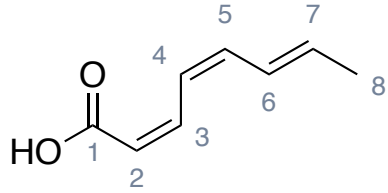

Carbon	δ_C (ppm) literature	δ_C (ppm) experimental	$\Delta\delta_C$ (ppm)
1	172.3	170.0	2.3
2	116.0	118.3	2.3
3	141.0	140.3	0.7
4	126.0	127.6	1.6
5	138.7	138.8	0.1
6	122.0	123.4	1.4
7	136.1	136.4	0.3
8	18.7	18.8	0.1

6. IR Spectra

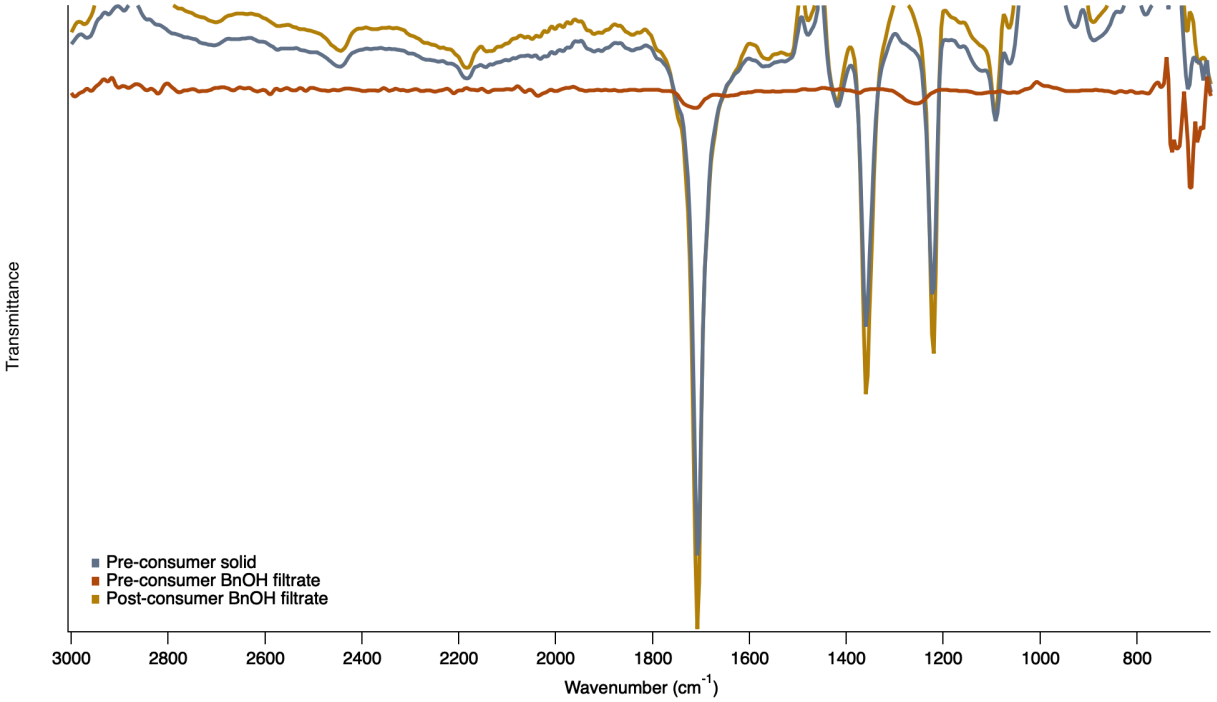

Figure S13. IR spectra of pretreatment solid fragments from pre-consumer composite (blue), pretreatment solution from pre-consumer composite in benzyl alcohol (red), and pretreatment solution from post-consumer composite in benzyl alcohol (yellow).

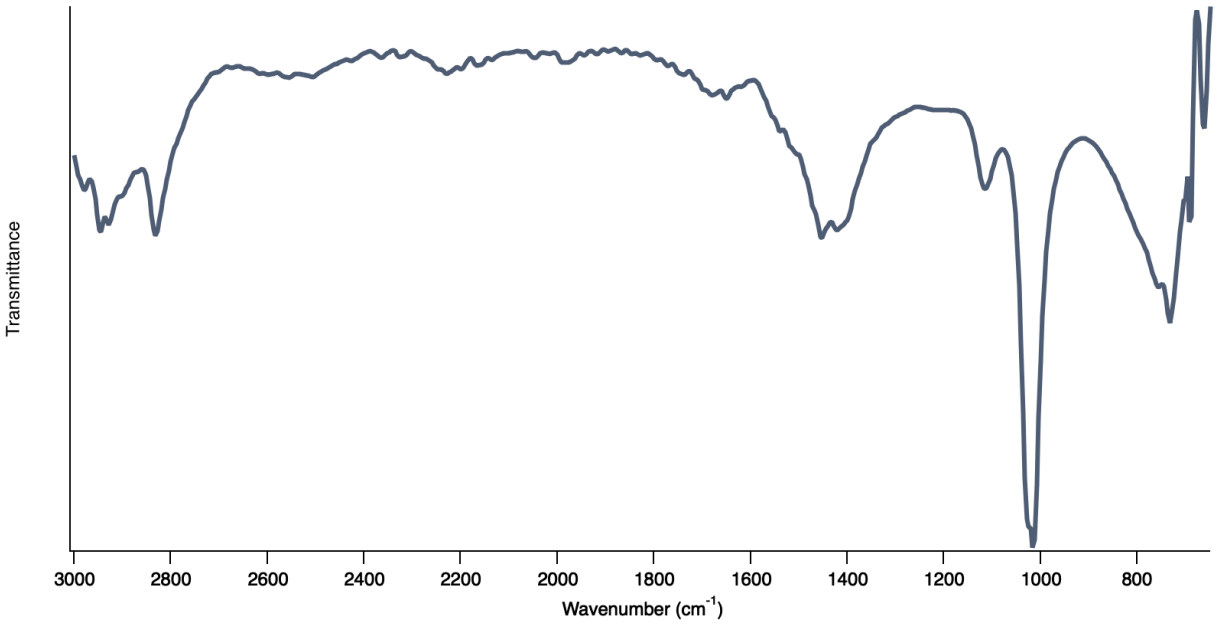

Figure S14. IR spectrum of (2Z,4Z,6E)-octa-2,4,6-trienoic acid in methanol.

7. NMR Spectra

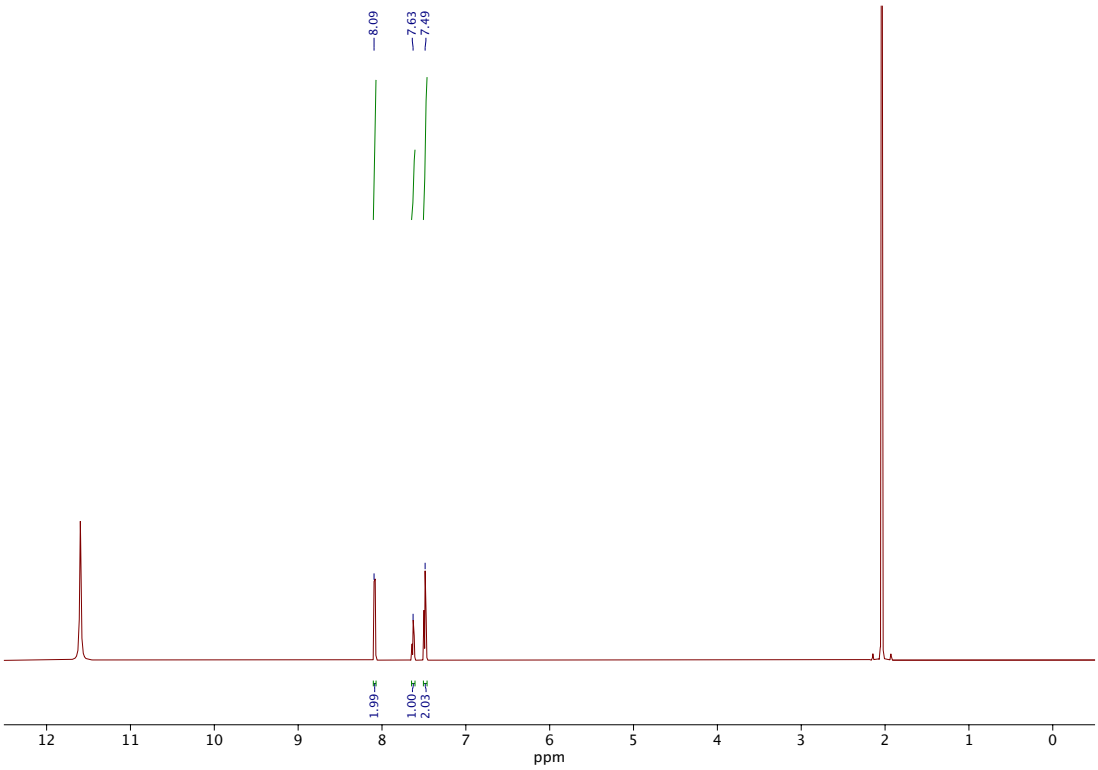

Figure S15. ^{1}H NMR (600 MHz) spectrum of isolated benzoic acid from pre-consumer composite digest in AcOH-d_4.

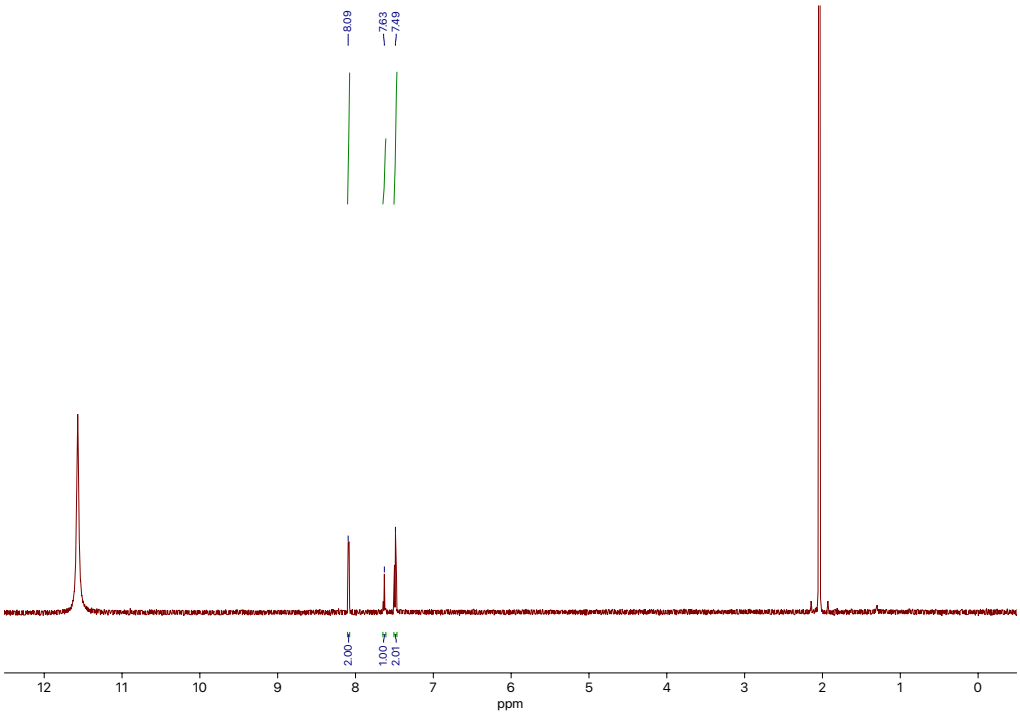

Figure S16. ^{1}H NMR (600 MHz) spectrum of isolated benzoic acid from post-consumer composite digest in AcOH-d_4.

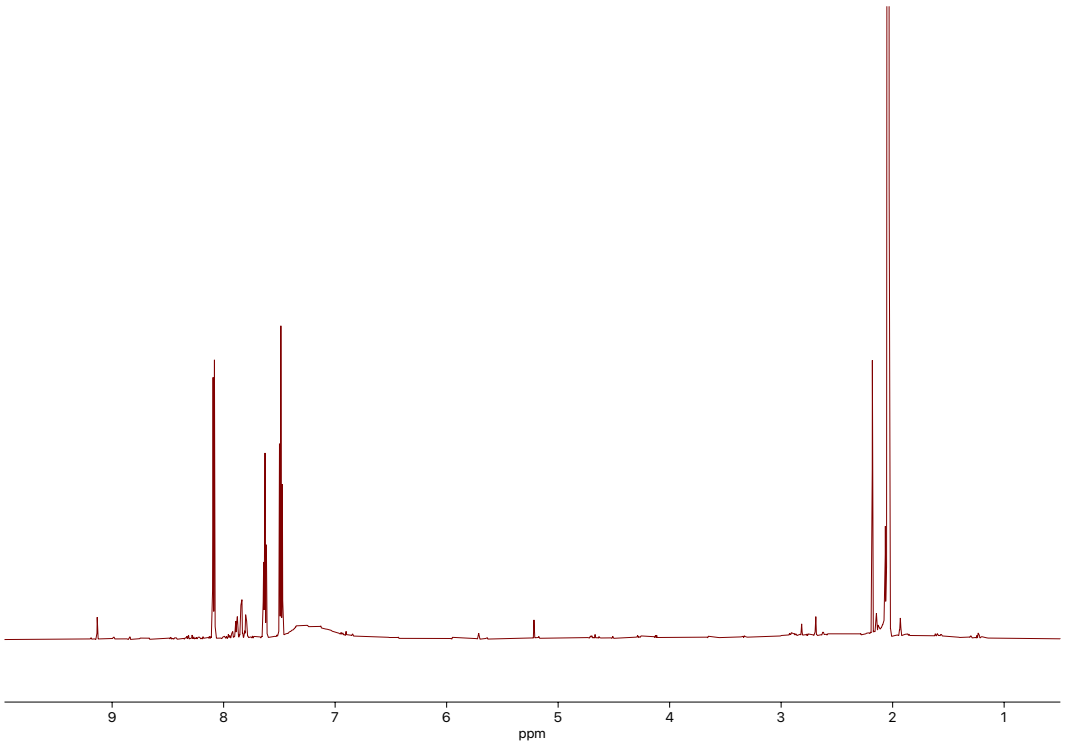

Figure S17. ^{1}H NMR (600 MHz) spectrum of oligomers from pre-consumer (FiberGlast Part #77 Polyester Molding Resin) composite digest in AcOH-d_4.

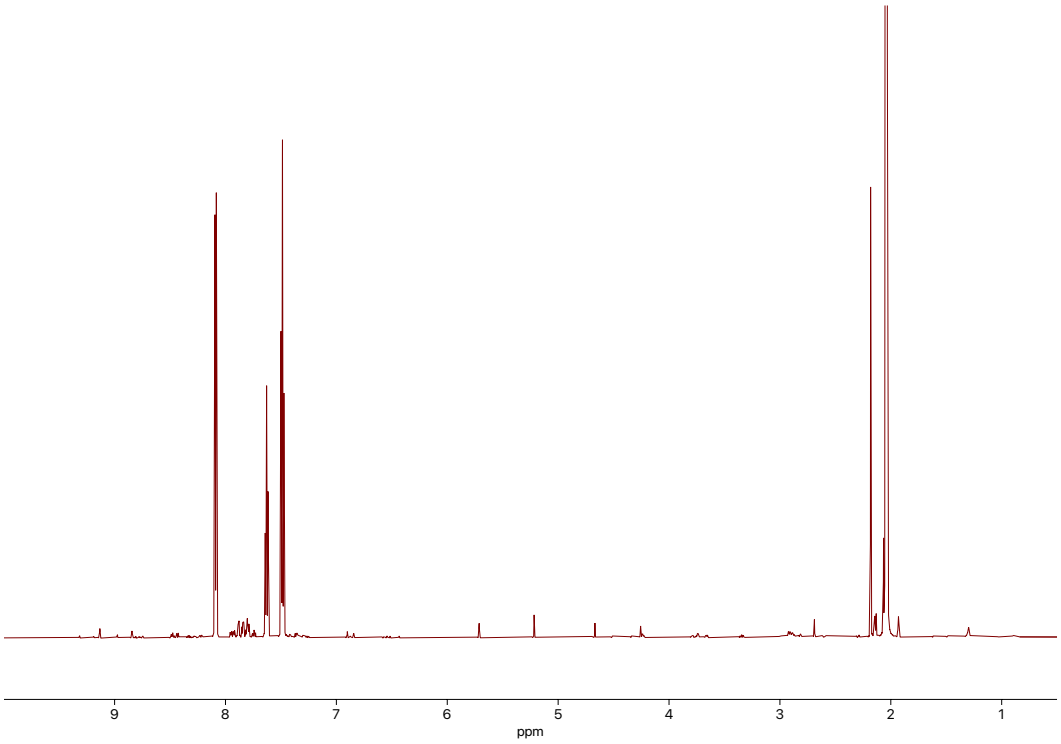

Figure S18. ^{1}H NMR (600 MHz) spectrum of impurities removed via recrystallization of benzoic acid isolated from pre-consumer (FiberGlast Part #77 Polyester Molding Resin) composite digest in AcOH-d_4.

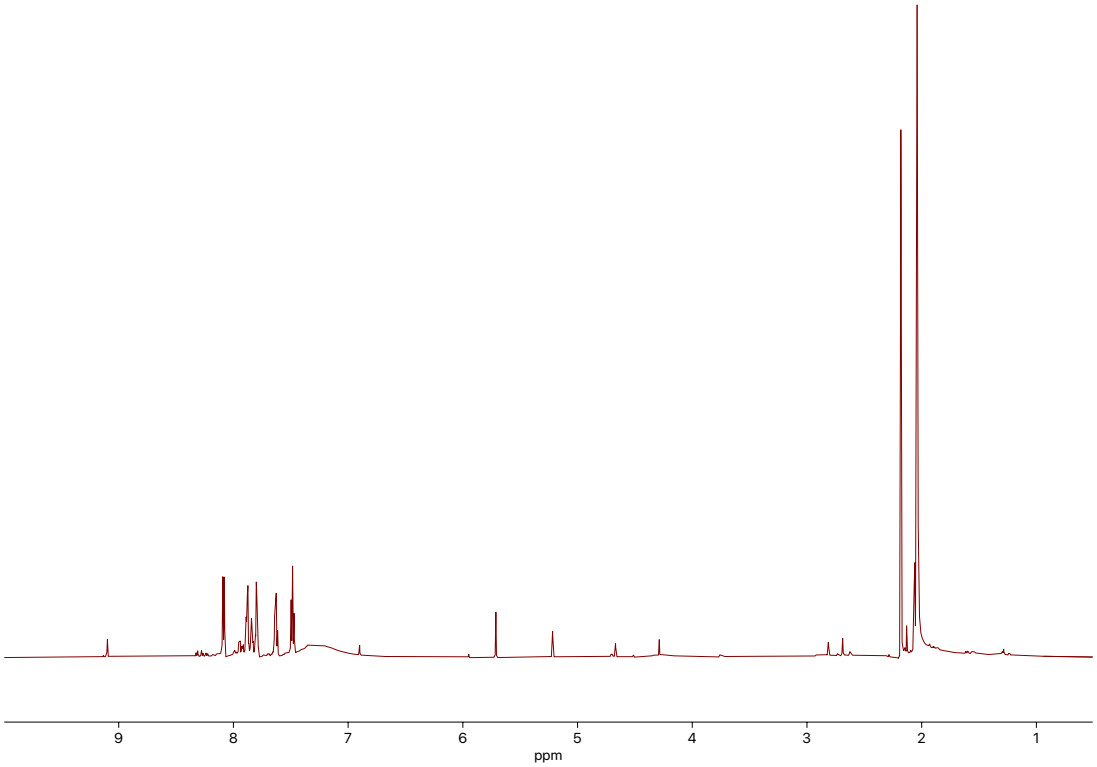

Figure S19. ^{1}H NMR (600 MHz) spectrum of oligomers from pre-consumer (FiberGlast Part #78 – Laminating Resin AropolTM L 67355 T-20 TS) composite digest in AcOH-d_4.

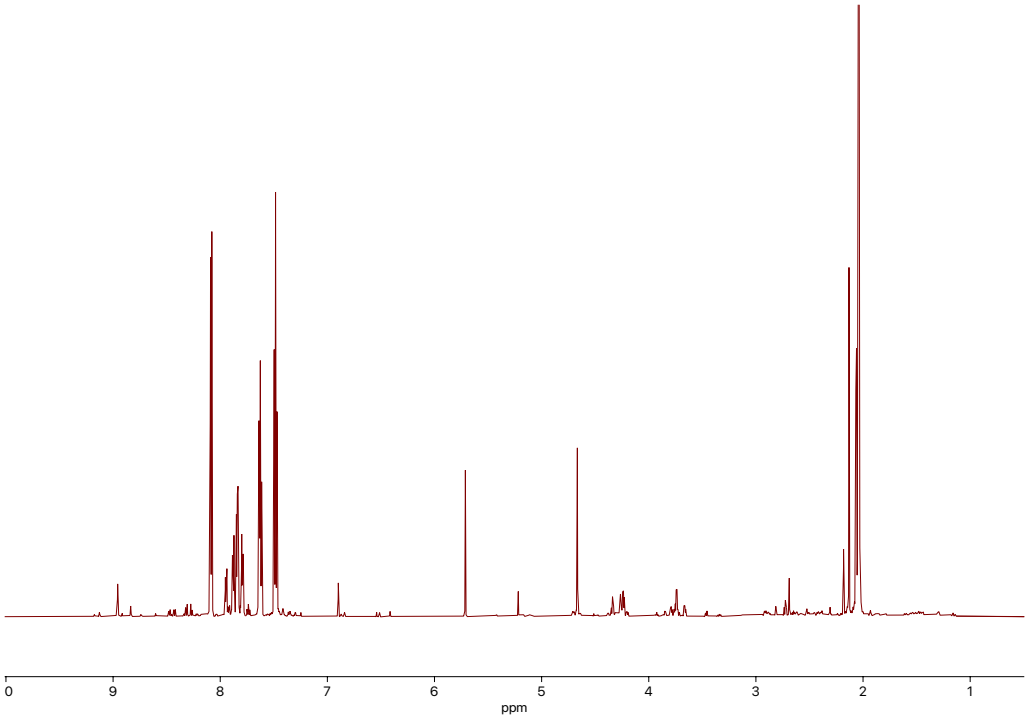

Figure S20. ^{1}H NMR (600 MHz) spectrum of impurities removed via recrystallization of benzoic acid isolated from pre-consumer (FiberGlast Part #78 – Laminating Resin AropolTM L 67355 T-20 TS) composite digest in AcOH-d_4.

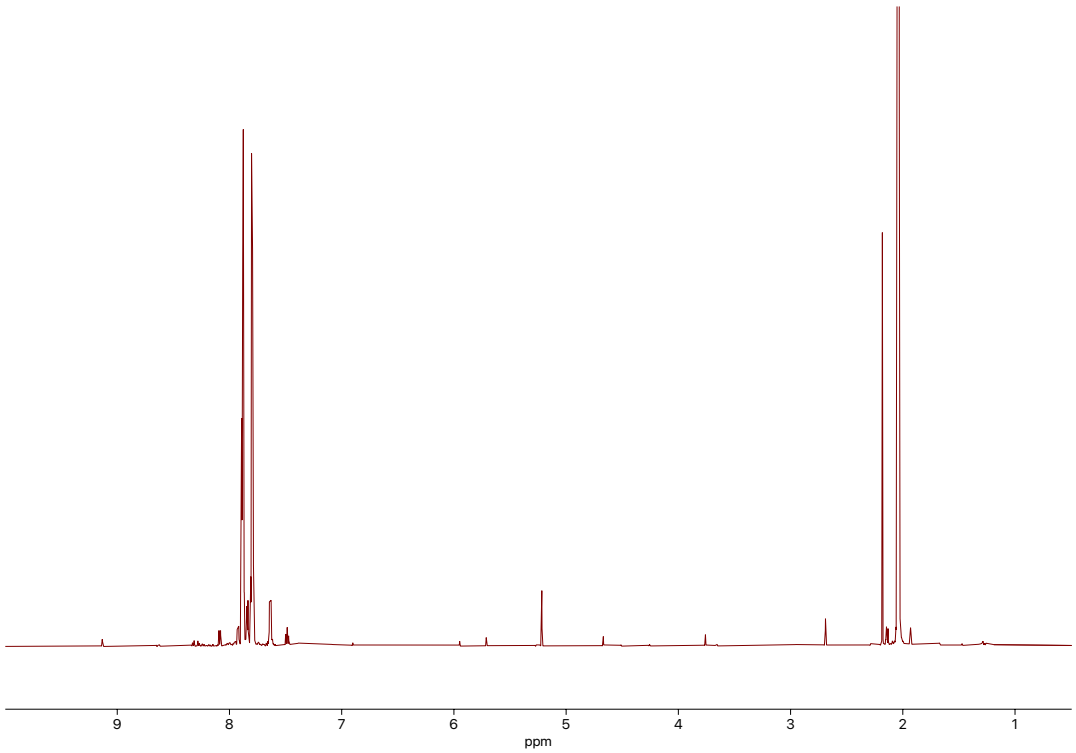

Figure S21. ^{1}H NMR (600 MHz) spectrum of oligomers from post-consumer composite digest in AcOH-d_4.

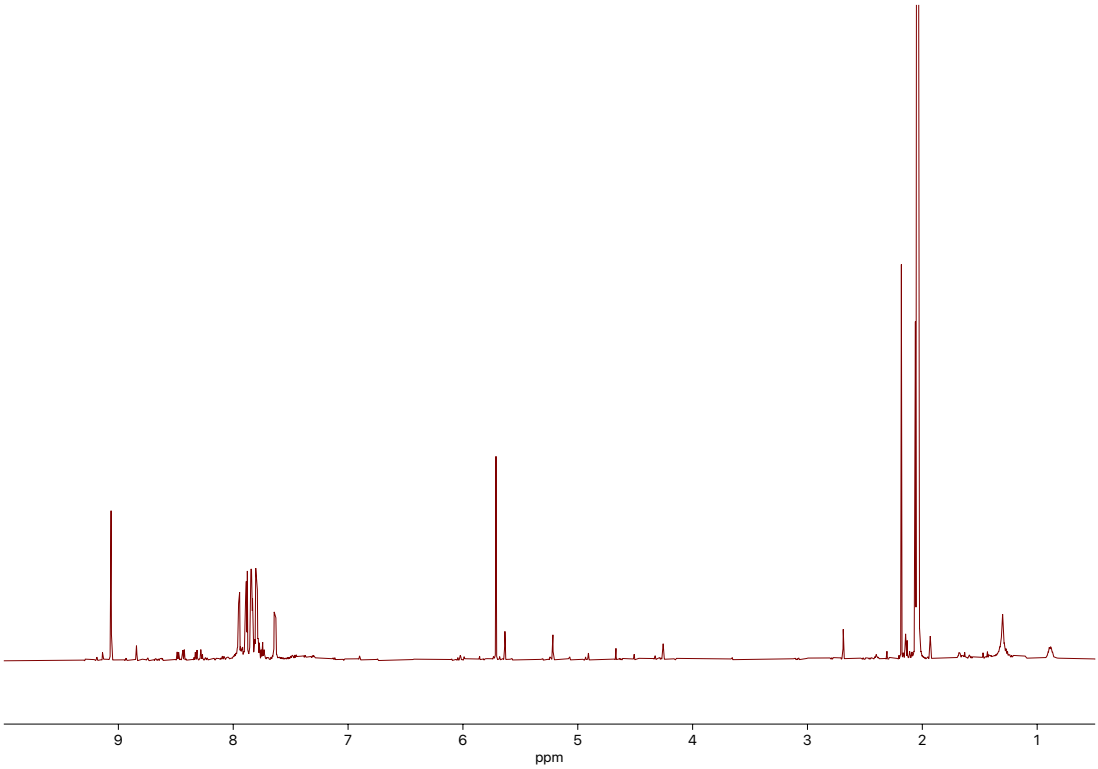

Figure S22. ^{1}H NMR (600 MHz) spectrum of impurities removed via recrystallization of benzoic acid isolated from post-consumer composite digest in AcOH-d_4.

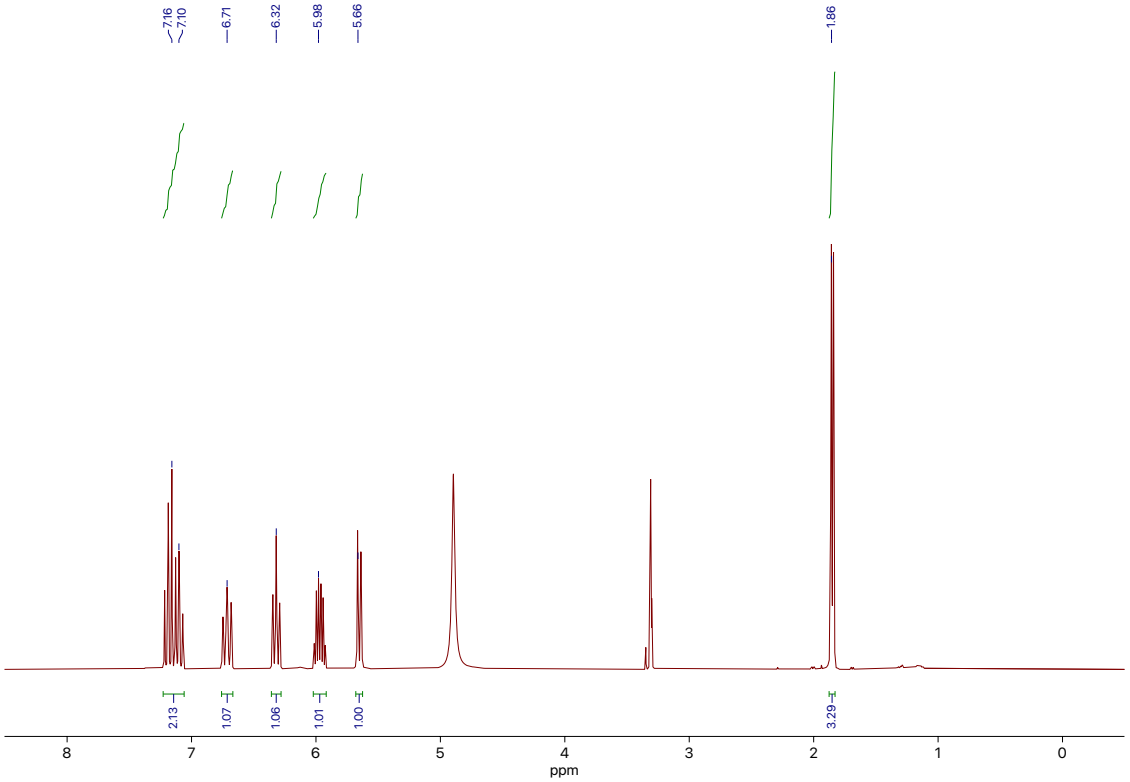

Figure S23. ^{1}H NMR (400 MHz) spectrum of purified (2Z,4Z,6E)-octa-2,4,6-trienoic acid in MeOH-d_4.

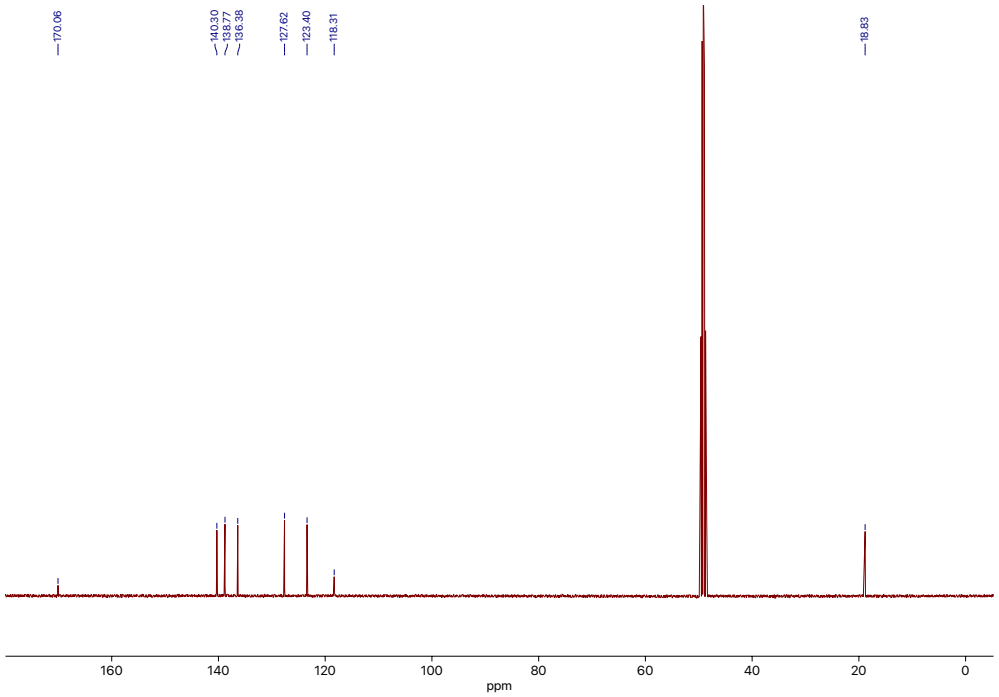

Figure S24. ^{13}C{^{1}H} NMR spectrum of purified (2Z,4Z,6E)-octa-2,4,6-trienoic acid in MeOH-d_4.

8. UV-vis Spectrum

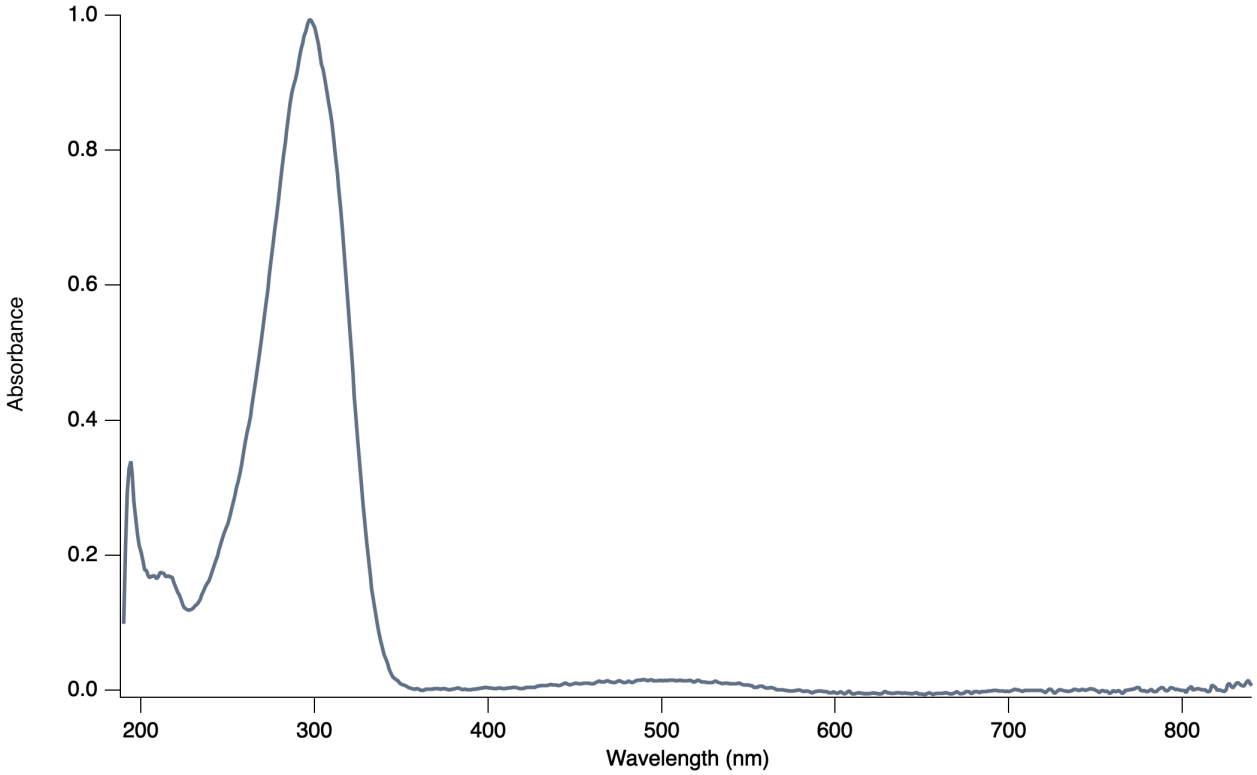

Figure S25. UV-vis spectrum of (2Z,4Z,6E)-octa-2,4,6-trienoic acid in methanol.

9. References

1. Hutner, S.H.; Provasoli, L.; Schatz, Albert; Haskins, C. Some Approaches to the Study of the Role of Metals in the Metabolism of Microorganisms. *Proc. Am. Philos. Soc.* **1950**, *94*, 152–170.
2. Brown, D. W.;Yu, J. H.; Kelkar, H. S.; Fernandes, M.; Nesbitt, T. C.; Keller, N. P.; Adams, T. H.; Leonard, T. J. Twenty-five coregulated transcripts define a sterigmatocystin gene cluster in *Aspergillus nidulans*. *Proc. Natl. Acad. Sci. USA* **1996**, *93*, 1418–1422.
3. Chiang, Y. *et al.* Molecular Genetic Mining of the *Aspergillus* Secondary Metabolome: Discovery of the Emericellamide Biosynthetic Pathway. *Chem. Biol.* **2008**, *15*, 527–532.
4. Chiang, Y. *et al.* A Gene Cluster Containing Two Fungal Polyketide Synthases Encodes the Biosynthetic Pathway for a Polyketide, Asperfuranone, in *Aspergillus nidulans*. *J. Am. Chem. Soc.* **2009**, *131*, 2965–2970.
5. Szewczyk, E. *et al.* Fusion PCR and gene targeting in *Aspergillus nidulans*. *Nat. Protoc.* **2006**, *1*, 3111–3120.
6. Jang, J. & Yang, H. The effect of surface treatment on the performance improvement of carbon fiber/polybenzoxazine composites. *J. Mater. Sci.* **2000**, *35*, 2297–2303.
7. Langston, T. A. & Granata, R. D. Influence of nitric acid treatment time on the mechanical and surface properties of high-strength carbon fibers. *J. Compos. Mater.* **2014**, *48*, 259–276.
8. Chen, X., Wang, X. & Fang, D. A review on C1s XPS-spectra for some kinds of carbon materials. *Fullerenes, Nanotub. Carbon Nanostructures* **2020**, *28*, 1048–1058.
9. Grau, M. F. *et al.* Hybrid Transcription Factor Engineering Activates the Silent Secondary Metabolite Gene Cluster for (+)-Asperlin in *Aspergillus nidulans*. *ACS Chem. Biol.* **2018**, *13*, 3193−3205.